Journal of Sound and Vibration (1999) **227**(3), 611–645
Article No. jsvi.1999.2354, available online at http://www.idealibrary.com on IDEAL®

SOME CONSIDERATIONS ON THE BASIC ASSUMPTIONS IN ROTORDYNAMICS

G. Genta, C. Delprete and E. Busa

Department of Mechanics, Politecnico di Torino, Corso Duca degli Abruzzi 24, 10129 *Torino, Italy*

(*Received* 20 *January* 1999, *and in final form* 6 *May* 1999)

The dynamic study of rotors is usually performed under a number of assumptions, namely small displacements and rotations, small unbalance and constant angular velocity. The latter assumption can be substituted by a known time history of the spin speed. The present paper develops a general non-linear model which can be used to study the rotordynamic behaviour of both fixed and free rotors without resorting to the mentioned assumptions and compares the results obtained from a number of non-linear numerical simulations with those computed through the usual linearized approach. It is so possible to verify that the validity of the rotordynamic models extends to situations in which fairly large unbalances and whirling motions are present and, above all, it is shown that the doubts forwarded about the application of a model which is based on constant spin speed to the case of free rotors in which the angular momentum is constant have no ground. Rotordynamic models can thus be used to study the stability in the small of spinning spacecrafts and the insight obtained from the study of rotors is useful to understand their attitude dynamics and its interactions with the vibration dynamics.
© 1999 Academic Press

1. INTRODUCTION

The dynamic study of rotors is usually performed under the assumptions of small displacements and rotations. Moreover, the angular velocity is assumed to be constant, or at least a known function of time. These assumptions allow a number of linearizations of both the inertial and the elastic terms in the equations of motion.

The assumptions of small displacements and rotations are retained even when studying the behaviour of non-linear rotors, the non-linearities being usually ascribed to bearings (of the fluid, rolling elements or even magnetic type), dampers or other causes, as the presence of cracks.

Rotors are defined by ISO as bodies rotating about a fixed axis, constrained to do so by cylindrical hinges. However, this is not in general necessary and there are cases in which there are no constraints, as in the case of spinning spacecrafts or celestial bodies, which can after all be considered as rotors. They are often defined as "free" rotors, as opposed to the more conventional "fixed" rotors, supported in bearings [1].

0022-460X/99/430611 + 35 $30.00/0 © 1999 Academic Press

While the presence of the bearings does not change the nature of the problem (in the case of the Jeffcott rotor it is possible to show that there is no difference between the cases of a flexible rotor on stiff bearings or of a stiff rotor on compliant bearings, at least if only the elasticity of the system is considered) the displacements can be far greater in the case of "free" rotors and this makes the small displacements and, above all, small rotations assumptions more problematic. Moreover, while in the case of "fixed" rotors the spin speed is assumed to be constant (or, more generally, a known function of time), free rotors are usually studied under the assumption of constant angular momentum. So spinning spacecraft attitude dynamics and rotordynamics are usually seen as two separate branches of dynamics, each one with its own notation, distinctive approach and limitations [2–6].

Spacecraft attitude dynamics usually deals with single rigid bodies or with multibody systems, in which the inertial properties of only one of them is considered as relevant for the study of the dynamic behaviour of the spacecraft [5]. For the attitude and guidance control, the spacecraft is assumed to be a single rigid body, with its flexible parts not affecting significantly the overall dynamic behaviour of the vehicle.

However, spacecrafts made of several bodies with relevant mass and moments of inertia connected through very compliant structural element, as is the case of recently proposed satellites for flight experiments on fundamental physics (MiniSTEP [7], GG [8]) and large space stations (ISS [9]), require a reconsidering of this assumption. The low stiffness (or better, the low value of the natural frequency) causes the attitude dynamics to be coupled to the vibration dynamics; such coupling can make the vibration isolation of the payload more difficult and, above all, can cause stability problems.

This issue is usually taken into account using multibody dynamics codes (for example, DCAP code [10]), which are based on the numerical integration in time of a complete nonlinear model of the system. They allow to simulate the spacecraft attitude and vibration dynamics in detail, but this interaction is still difficult to investigate in a general way.

The experience in the field of conventional "fixed" rotors can help in clarifying some of these aspects, provided that the consequences of the assumptions of small displacements and, above all, of constant spin speed, which are usually done in rotordynamics, are fully understood. In particular, there have been claims that the violation of the conservation of the angular momentum linked with the constant speed assumption of rotordynamics makes the models based on the latter unable to study the stability of free rotors even in the small [11].

The present authors studied the dynamics and the stability in the small of a proposed satellite for a fundamental physics flight experiment [12, 13], using the conventional approach of linearized rotordynamics in previous papers [14]. An interesting technical evaluation of the above proposal has been performed by ESTEC, and published in reference [11].

These studies highlighted some critical issues.

The concepts of critical speeds and of self-centring, well known in the case of supported rotors, apply as well to the multibody free rotors, due to the presence of

elastic and damped connections between the carrier and the inner masses of the system.

The role of damping (nonrotating, rotating, synchronous) on the stability of multibody rotors can be fully understood only if studied with reference to a frame fixed to the element in which the energy dissipation occurs. This is usually done for fixed rotors, where non-rotating (statoric) elements are present, while it was often neglected in the case of free rotors, where all parts typically rotate [5]. Stabilization can occur by adding non-synchronous rotating damping [15], even if it is often problematic from the practical point of view [11]. The authors propose to use active dampers, which are able to synthesize non-rotating (or generally non-synchronous) damping even if they are physically rotating together with the rotor. Also gyroscopic effects play a relevant role on the attitude behaviour of the spacecraft and in the coupling between attitude and vibration dynamics.

The aim of the present study is to clarify the above-mentioned issues, investigating on the basic approximations typical of rotordynamics and on the respective roles of the assumptions of constant speed and constant angular momentum.

2. SINGLE-RIGID-BODY FIXED ROTOR

2.1. EQUATIONS OF MOTION

Consider a rigid body rotating about two cylindrical hinges located on one of its principal axes of inertia (z-axis) and assume that the ellipsoid of inertia is round, i.e., its moments of inertia in a plane perpendicular to the rotation axis are equal (Figure 1). Assume that the centre of mass G is not exactly coincident with point C, located on the axis connecting the two bearings, and that its eccentricity ε lies, for simplicity, on its x-axis. This does not detract from the generality of the model, as the body is axi-symmetrical. No couple unbalance is assumed. Let J_p and J_t be, respectively, the moments of inertia about the baricentrical principal axis, which

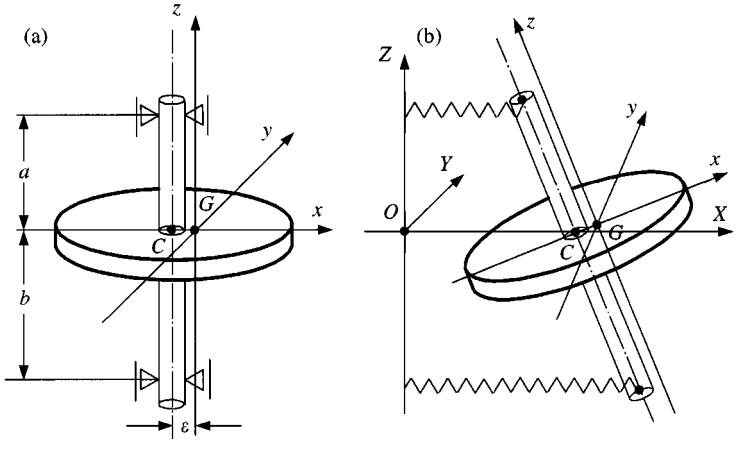

Figure 1. Single-rigid-body fixed rotor; sketch of the system (a) and deflected configuration (b).

coincides with the rotation axis but for the eccentricity ε, and any axis in the rotation plane.

Assume that the elastic and damping behaviour of the bearings is linear and isotropic, with stiffness k and damping c. This implies that the axial stiffness is equal to the radial one, but this does not constitute a limitation of the present model. If the usual assumptions of small displacements and rotations are made, the lateral, axial and torsional behaviours can be shown to be uncoupled and the former can be studied by resorting to four degrees of freedom, which can be coupled two by two in just two complex co-ordinates. The model coincides, apart from the couple unbalance here neglected, with the four-degrees-of-freedom model described in reference [16]. The dynamic study can be performed in the same way, but without resorting to any linearization.

The reference frames, the choice of the six generalized co-ordinates and the general equations of motion are described in Appendix A. Note that there is a difference between the present approach and the one described in reference [16]: to avoid overwhelming complexities in the differentiation of the kinetic energy, here the generalized co-ordinates used to study translational motions are those of the centre of mass G instead those of the geometrical centre of the shaft C.

By solving the last equation (A10) (see Appendix A) in $\ddot{\theta}$, substituting it into the first one, and stating that the body is axially symmetrical ($J_x = J_y = J_t$), the final form of the equations of motion is

$$
\begin{aligned}
\ddot{X} &= \frac{Q_X}{m},\\
\ddot{Y} &= \frac{Q_y}{m},\\
\ddot{Z} &= \frac{Q_z}{m},\\
\ddot{\varphi}_X &= -\left(\frac{J_p}{J_t} - 2\right)\tan(\varphi_y)\dot{\varphi}_y\dot{\varphi}_X - \frac{J_p}{J_t\cos(\varphi_y)}\dot{\theta}\dot{\varphi}_y + \frac{Q_{\varphi X} - \sin(\varphi_y)Q_\theta}{J_t\cos^2(\varphi_y)},\\
\ddot{\varphi}_y &= \left(\frac{J_p}{J_t} - 1\right)\sin(\varphi_y)\cos(\varphi_y)\dot{\varphi}_X^2 + \frac{J_p}{J_t}\cos(\varphi_y)\dot{\theta}\dot{\varphi}_X + \frac{Q_{\varphi_y}}{J_t},\\
\ddot{\theta} &= -\sin(\varphi_y)\ddot{\varphi}_X - \cos(\varphi_y)\dot{\varphi}_y\dot{\varphi}_X + \frac{Q_\theta}{J_p}.
\end{aligned}
\tag{1}
$$

The generalized forces due to the bearings are readily obtained from equations (A25)–(A30) (for the elastic terms) and from equation (A36) (for the damping terms), remembering that the coordinates of the points in which the bearings are located on the rotor (expressed in the rotor-fixed frame) are (Figure 1):

$$[-\varepsilon\ \ 0\ \ a]^{\mathrm{T}}, \qquad [-\varepsilon\ \ 0\ \ -b]^{\mathrm{T}}$$

and those of the corresponding points of the stator are, in the inertial frame

$$[0\ \ 0\ \ a]^{\mathrm{T}}, \qquad [0\ \ 0\ \ -b]^{\mathrm{T}}.$$

It is easy to verify that equations (1) can be linearized, under the assumption of small displacements X, Y and Z, small rotations φ_X and φ_y while rotation θ and the spin speed $\dot{\theta}$ are arbitrary large, and small unbalance ε, obtaining

$$m\ddot{X} + C_{11}[\dot{X} + \varepsilon\dot{\theta}\sin(\theta)] + C_{12}\dot{\varphi}_y + K_{11}[X - \varepsilon\cos(\theta)] + K_{12}\varphi_y = 0,$$

$$m\ddot{Y} + C_{11}[\dot{Y} - \varepsilon\dot{\theta}\cos(\theta)] - C_{12}\dot{\varphi}_X + K_{11}[Y - \varepsilon\sin(\theta)] - K_{12}\varphi_X = 0,$$

$$m\ddot{Z} + C_{11}\dot{Z} + K_{11}Z = 0,$$

$$J_t\ddot{\varphi}_X + J_p\dot{\theta}\dot{\varphi}_y - C_{21}[\dot{Y} - \varepsilon\dot{\theta}\cos(\theta)] + C_{22}\dot{\varphi}_X - K_{21}[Y - \varepsilon\sin(\theta)] + K_{22}\varphi_X = 0,$$

$$J_t\ddot{\varphi}_y - J_p\dot{\theta}\dot{\varphi}_X + C_{21}[\dot{X} + \varepsilon\dot{\theta}\sin(\theta)] + C_{22}\dot{\varphi}_y + K_{21}[X - \varepsilon\cos(\theta)] + K_{22}\varphi_y = 0,$$

$$\ddot{\theta} = 0, \tag{2}$$

where

$$\mathbf{C} = c\begin{bmatrix} 2 & a-b \\ a-b & a^2+b^2 \end{bmatrix}, \qquad \mathbf{K} = k\begin{bmatrix} 2 & a-b \\ a-b & a^2+b^2 \end{bmatrix}.$$

Apart from the differences due to referring the equations of motion to point G instead of point C, equations (2) are those commonly used in linearized rotordynamics. It is easy to verify that the uncoupling between axial, torsional and lateral behaviour holds and that the last equation states that the angular velocity $\dot{\theta}$ is constant. In the linearized system there is no difference between constant angular momentum and constant spin speed.

As the system is damped and unbalanced, there is energy dissipation in the bearings (even if they are assumed to be frictionless) due to the whirling motion. If this effect is accounted for, the last equation of motion becomes

$$\ddot{\theta} + \omega^2\,\Im\{\bar{\mathbf{F}}^{\mathrm{T}}[\omega^4(\mathbf{M} - \mathbf{G}) + \mathrm{i}\omega\mathbf{C} + \mathbf{K}]^{-1}\mathbf{F}\} = 0, \tag{3}$$

where the symbols are referred to the complex notation for steady state whirling as described in reference [17]. The term expressing the rotordynamic drag in the bearings is then quadratic in the eccentricity (included in vector $\mathbf{F}$), which is a small parameter, and hence in a linearized model it should be dropped. However, it will be retained in the following numerical simulations to show the importance of such phenomenon in practical applications.

2.2. NUMERICAL SIMULATIONS

The number of independent parameters involved in the equations of motion is large and hence it is impossible to draw general conclusions: only a few numerical simulations will be reported here.

TABLE 1

Some results of the simulation of the behaviour of a fixed rotor with different values of the eccentricity and at different speeds close to the critical speed. The radius of the orbit, the speed reduction $\Delta\omega$ in 1 s *and the amplitude of the axial displacement* z_{max} *are reported*

ε [μm]	ω [r.p.m.]	Orbit radius [μm]		$\Delta\omega/\omega$ (in 1 s)		z_{max} [μm]	
		Linear	Nonlin.	Linear	Nonlin.	Linear	Nonlin.
1	9000	28·8	28·8	$0{\cdot}94\times10^{-6}$	$1{\cdot}12\times10^{-6}$	0	$1{\cdot}14\times10^{-4}$
	9200	42·6	42·6	$2{\cdot}11\times10^{-6}$	$2{\cdot}35\times10^{-6}$	0	$3{\cdot}07\times10^{-4}$
100	9000	2880	2880	$6{\cdot}8\times10^{-3}$	$7{\cdot}7\times10^{-3}$	0	1·14
	9200	4260	4260	$21{\cdot}1\times10^{-3}$	$23{\cdot}5\times10^{-3}$	0	3·08
1000	9000	28 800	28 800	0·074	0·074	0	114
	9200	45 500	44 200	0·094	0·108	0	308

Consider a rigid rotor with the following characteristics: mass $m = 10$ kg, moments of inertia $J_t = 0{\cdot}1$ kgm^2, $J_p = 0{\cdot}15$ kgm^2, distances between the bearings and the centre of mass $a = 100$ mm and $b = 200$ mm, stiffness and damping of the bearings $k = 5\times10^6$ N/m and $c = 100$ Ns/m respectively. The linearized analysis yields a single critical speed at 957·0 rad/s (9139 r.p.m.) and two natural frequencies at standstill are equal to 921·2 rad/s (146·6 Hz) and 1628 rad/s (259·1 Hz).

Three values of the eccentricity were considered, namely $\varepsilon = 1$, 100 μm and 1 mm. Assuming a maximum speed of 20 000 r.p.m., they correspond to balancing grades equal to 2, 200 and 2000: the first one is a fairly accurate balancing, as common in gas turbines, the second is a rough balancing, as for crankshafts of car engines, while the third is so rough not to be included in ISO 1940 standards. Actually the last value, corresponding to an unbalance of 10 000 gmm, is too high for any practical application; it has been chosen as a sort of limiting case.

The simulations were performed at speeds close to the critical speed, one slightly lower (942·5 rad/s = 9000 r.p.m.) and one slightly higher (963·4 rad/s = 9200 r.p.m.). A standard fourth order Runge–Kutta algorithm with adaptative timestep has been used for all the simulations reported in the present paper. As stability problems were never encountered, no attempt to improve the integration routine was performed. Some typical results are reported in Table 1.

In the case of small unbalance (1 μm) the results from the non-linear model are practically coincident with those obtained from the linearized theory. The slowing down of the rotor is almost negligible, and close to that predicted by the linearized model and the amplitude of the axial vibration is very small: the flexural-torsional and flexural-axial coupling is then completely negligible.

Also in the case of the intermediate unbalance (100 μm) the results obtained are still close to those obtained from the linearized model, as also shown by the increase of the orbit radius which is proportional to the increase of eccentricity. The

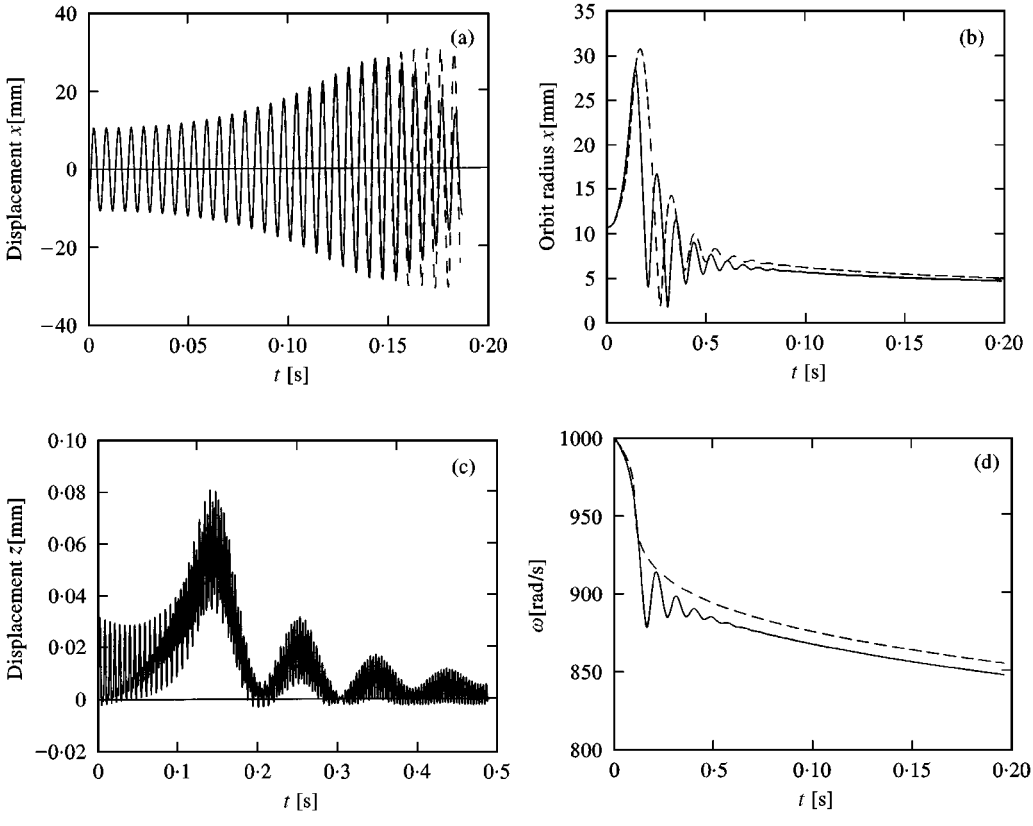

Figure 2. Single-rigid-body fixed rotor; results of the numerical simulation with an eccentricity of 1 mm and initial speed of 9200 r.p.m. Time history of (a) lateral displacement in x-direction; (b) radius of the orbit; (c) axial displacement, —— non-linear – – – linear and (d) spin speed.

amplitude of the axial vibration is still negligible and the slowing down, although no more negligible, is still small and close to that predicted by equation (3): the flexural-torsional and flexural-axial coupling is still negligible.

With the largest value of the unbalance (1 mm) the rotor slows down at a quite high rate as much energy is dissipated by the supports. When the initial spin speed is higher than the critical speed the rotor slows down quickly and enters the subcritical regime with a sudden drop in speed (see Figure 2, in which an initial speed of 1000 rad/s has been assumed). The radius of the orbit oscillates in time during the critical speed crossing as described in reference [17]. However, even in this case, the time history of the lateral displacement is close to that computed using the linearized model, and the amplitude of the axial displacement is small if compared with that of the lateral one (about 0·26%), showing a very weak flexural-axial coupling. The time history of the speed shows that a certain flexural-torsional coupling is present, as the system undergoes some torsional oscillations which are not predicted by the linearized model (equation (3)); however the approximation of the linearized model is generally not bad even for the decrease of speed. The time histories of the orbit amplitude computed using the nonlinear and the linearized models cannot be compared directly, as they are much influenced

by the decrease of the spin speed, but the latter model still yields reasonable results, even if the amplitude is definitely very large.

The example shows that the usual linearized model is still applicable in case of large unbalances and large whirling orbits. Note that the simulations have been performed in the worst conditions, i.e., with an unrealistically high unbalance and at speeds very close to the critical speed (in Figure 2 the critical speed is actually crossed).

3. TWIN-RIGID-BODIES FREE ROTOR

3.1. EQUATIONS OF MOTION

Consider a free rotor made of two rigid bodies connected by springs and dampers. Assume that the centres of mass of the two bodies are coincident in the undeflected position and that they are linked together by six linear springs and viscous dampers arranged in the way shown in Figure 3. The values of the stiffness and the damping coefficient of the links located on the x- and y-axis are equal, in such a way that the system possesses axial symmetry. Also the inertial properties of the two rigid bodies are axially symmetrical and, as a consequence, the equations of motion of each one of them take the form of equation (1).

The two bodies are assumed to be perfectly balanced, i.e., the geometrical centre of the connection system coincides with the mass centre and the principal axes of inertia coincide with the principal axes of elasticity. By inspecting equation (1) and computing the generalized forces through equations (A14)–(A23) and equation (A36), it is possible to see that translational motions are uncoupled from rotational ones in the linearized and semi-linearized models, while in case of the non-linear one they are coupled only by the damping terms.

The general form of the 12 equations of motion is that of equations (1), written with subscripts 1 and 2 for the generalized co-ordinates, forces and system parameters. The generalized forces can be computed from the formulae reported in

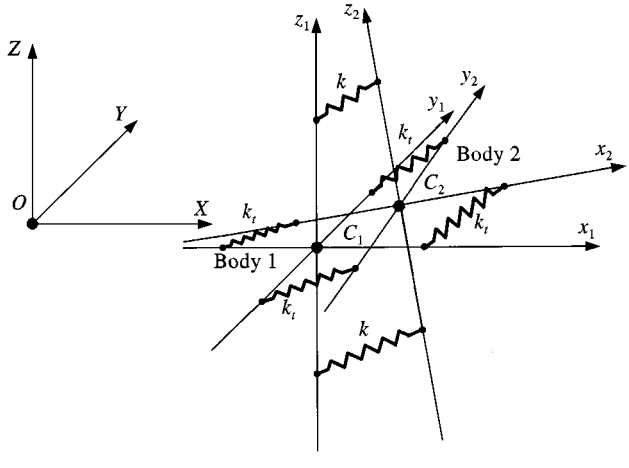

Figure. 3. Twin-rigid-bodies rotor; position of the springs and dampers.

Appendix A by simply introducing the co-ordinates of points P_1 and P_2 desumed from Figure 3 (there are six pairs of such points) into the equations and adding the results. For the forces due to the springs this procedure yields

$$Q_{X_1} = (4k_t + 2k)(X_2 - X_1), \tag{4}$$

$$Q_{Y_1} = (4k_t + 2k)(Y_2 - Y_1), \tag{5}$$

$$Q_{Z_1} = (4k_t + 2k)(Z_2 - Z_1), \tag{6}$$

$$\begin{aligned} Q_{\varphi_{X_1}} = {} & 2\{ka^2\cos(\varphi_{y_2})\cos(\varphi_{y_1}) + k_t b^2\cos(\theta_2 - \theta_1)[1 + \sin(\varphi_{y_2})\sin(\varphi_{y_1})]\} \\ & \times\sin(\varphi_{x_2} - \varphi_{x_1}) + 2k_t b^2\sin(\theta_2 - \theta_1)[\sin(\varphi_{y_2}) + \sin(\varphi_{y_1})]\cos(\varphi_{x_2} - \varphi_{x_1}), \end{aligned} \tag{7}$$

$$\begin{aligned} Q_{\varphi_{y_1}} = {} & 2ka^2[\sin(\varphi_{y_2})\cos(\varphi_{y_1}) - \cos(\varphi_{y_2})\sin(\varphi_{y_1})\cos(\varphi_{x_2} - \varphi_{x_1})] \\ & + 2k_t b^2\cos(\theta_2 - \theta_1)[\sin(\varphi_{y_2})\cos(\varphi_{y_1})\cos(\varphi_{x_2} - \varphi_{x_1}) - \cos(\varphi_{y_2})\sin(\varphi_{y_1})] \\ & - 2k_t b^2\sin(\theta_2 - \theta_1)\cos(\varphi_{y_1})\sin(\varphi_{x_2} - \varphi_{x_1}), \end{aligned} \tag{8}$$

$$\begin{aligned} Q_{\theta_1} = {} & 2k_t b^2\sin(\theta_2 - \theta_1)\{\cos(\varphi_{y_2})\cos(\varphi_{y_1}) + [1 + \sin(\varphi_{y_2})\sin(\varphi_{y_1})] \\ & \times\cos(\varphi_{x_2} - \varphi_{x_1})\} + 2k_t b^2\cos(\theta_2 - \theta_1)[\sin(\varphi_{y_2}) + \sin(\varphi_{y_1})]\sin(\varphi_{x_2} - \varphi_{x_1}), \end{aligned} \tag{9}$$

$$Q_{X_2} = -Q_{X_1}, \qquad Q_{Y_2} = -Q_{Y_1}, \qquad Q_{Z_2} = -Q_{Z_1}, \qquad Q_{\varphi_{x_2}} = -Q_{\varphi_{x_1}}, \tag{10–13}$$

$$\begin{aligned} Q_{\varphi_{y_2}} = {} & 2ka^2[\sin(\varphi_{y_1})\cos(\varphi_{y_2}) - \cos(\varphi_{y_1})\sin(\varphi_{y_2})\cos(\varphi_{x_2} - \varphi_{x_1})] \\ & + 2k_t b^2\cos(\theta_2 - \theta_1)[\sin(\varphi_{y_1})\cos(\varphi_{y_2})\cos(\varphi_{x_2} - \varphi_{x_1}) - \cos(\varphi_{y_1})\sin(\varphi_{y_2})] \\ & - 2k_t b^2\sin(\theta_2 - \theta_1)\cos(\varphi_{y_2})\sin(\varphi_{x_2} - \varphi_{x_1}), \end{aligned} \tag{14}$$

$$Q_{\theta_2} = -Q_{\theta_1}. \tag{15}$$

where a and b are the distances from the origin of the springs with stiffness k and k_t respectively.

The expressions of the generalized forces due to the dampers are more complex and the numerical simulations were performed using directly the expression of the damping matrix given by equation (A33).

It is possible to assume that, while the rotations of each invidual body are generally large, the differential rotations of one with respect to the other are small. Also, the differential displacements can be considered small. A model based on this assumption will be referred to as a semi-linearized model.

The generalized forces due to the springs and the dampers can now be computed in closed form, obtaining

$$\begin{aligned} Q_{X_1} = {} & (4k_t + 2k)(X_2 - X_1) + (4c_t + 2c)\{\dot{X}_2 - \dot{X}_1 + [(Y_2 - Y_1)\sin(\varphi_{X_1}) \\ & - (Z_2 - Z_1)\cos(\varphi_{X_1})]\dot{\varphi}_{y_1} + \cos(\varphi_{y_1})[(Y_2 - Y_1)\cos(\varphi_{X_1}) \\ & + (Z_2 - Z_1)\sin(\varphi_{X_1})]\dot{\theta}_1\} \end{aligned} \tag{16}$$

$$Q_{Y_1} = (4k_t + 2k)(Y_2 - Y_1) + (4c_t + 2c)\{\dot{Y}_2 - \dot{Y}_1 + (Z_2 - Z_1)\dot{\varphi}_{X_1} - (X_2 - X_1)\sin(\varphi_{X_1})\dot{\varphi}_{y_1} + [-(X_2 - X_1)\cos(\varphi_{X_1})\cos(\varphi_{y_1}) + (Z_2 - Z_1)\sin(\varphi_{y_1})]\dot{\theta}_1\} \tag{17}$$

$$Q_{Z_1} = (4k_t + 2k)(Z_2 - Z_1) + (4c_t + 2c)\{\dot{Z}_2 - \dot{Z}_1 - (Y_2 - Y_1)\dot{\varphi}_{X_1} + (X_2 - X_1)\cos(\varphi_{X_1})\dot{\varphi}_{y_1} - [(X_2 - X_1)\sin(\varphi_{X_1})\cos(\varphi_{y_1}) + (Z_2 - Z_1)\sin(\varphi_{y_1})]\dot{\theta}_1\} \tag{18}$$

$$Q_{\varphi_{X_1}} = 2\{ka^2\cos^2(\varphi_{y_1}) + k_t b^2[1 + \sin^2(\varphi_{y_1})]\}(\varphi_{x_2} - \varphi_{x_1}) + 4k_t b^2\sin(\varphi_{y_1})(\theta_2 - \theta_1) + 2\{ca^2\cos^2(\varphi_{y_1}) + k_t b^2[1 + \sin^2(\varphi_{y_1})]\}(\dot{\varphi}_{x_2} - \dot{\varphi}_{x_1}) + 2(ca^2 - 2c_t b^2)\sin(\varphi_{y_1})\cos(\varphi_{y_1})(\varphi_{x_1} - \varphi_{x_2})\dot{\varphi}_{y_1} + 4c_t b^2\sin(\varphi_{y_1})(\dot{\theta}_2 - \dot{\theta}_1) + 2(ca^2 + c_t b^2)\cos(\varphi_{y_1})(\varphi_{y_2} - \varphi_{y_1})\dot{\theta}_1, \tag{19}$$

$$Q_{\varphi_{y_1}} = 2(ka^2 + k_t b^2)(\varphi_{y_2} - \varphi_{y_1}) + 2(ca^2 + c_t b^2)(\dot{\varphi}_{y_2} - \dot{\varphi}_{y_1}) + 2(ca^2 + c_t b^2)\cos(\varphi_{y_1})(\varphi_{x_1} - \varphi_{x_2})\dot{\theta}_1, \tag{20}$$

$$Q_{\theta_1} = 4k_t b^2(\theta_2 - \theta_1) + 4k_t b^2\sin(\varphi_{y_1})(\varphi_{x_2} - \varphi_{x_1}) + 4c_t b^2(\dot{\theta}_2 - \dot{\theta}_1) + 4c_t b^2\sin(\varphi_{y_1})(\dot{\varphi}_{x_2} - \dot{\varphi}_{x_1}) - 4c_t b^2\cos(\varphi_{y_1})(\varphi_{x_2} - \varphi_{x_1})\dot{\varphi}_{y_1}, \tag{21}$$

$$Q_{X_2} = -Q_{X_1}, \qquad Q_{\varphi_{X_2}} = -Q_{\varphi_{X_1}}, \tag{22}$$

$$Q_{Y_2} = -Q_{Y_1}, \qquad Q_{\varphi_{y_2}} = -Q_{\varphi_{y_1}}, \tag{23}$$

$$Q_{Z_2} = -Q_{Z_1}, \qquad Q_{\theta_2} = -Q_{\theta_1}. \tag{24}$$

A further linearization yields the usual equations of rotordynamics. Also in this case, the two assumptions of constant spin speed and constant angular momentum coincide in the linearized model. Also, the unstabilizing effect of rotating damping is clearly present in the equations.

3.2 NUMERICAL SIMULATIONS

Owing to the large number of independent parameters, the only way to compare the results obtained through the full equations, the semi-linearized and the fully linearized approach is to perform a very large number of numerical simulations. Only four cases are reported here, to obtain some indications which can be shown to yield a good qualitative understanding of the effect of such assumptions. In all

cases, the values of the damping coefficients have been chosen in such a way that the rotational flexural and torsional vibrations are characterized by a damping ratio $\zeta = 0{\cdot}1$ (quality factor $Q \approx 5$). The relevant data are listed in Table 2.

The main results of the linearized analysis are reported in Tables 3 and 4, separately for translational and rotational modes, which are decoupled. The rotor has been considered at standstill and spinning at 1000 rad/s. Cases $n = 1$ and 2 refer to free rotors with polar moment of inertia larger than the transversal moment of inertia. As a consequence they have no critical speeds related to rotational modes, which are stable in the whole spin speed range.

Case 1 refers to a rotor with a stiff connection between the two bodies, i.e., with flexural natural frequencies at standstill far higher than the maximum spin speed. The linearized results at 1000 rad/s show that the rigid-body conical precessional motion, occurring at 1450 rad/s (i.e., at the frequency $\omega J_p/J_t$) is completely uncoupled from the mode involving relative motions of the two parts of the system. The former is very little damped, with a decay rate of about 10^{-8} 1/s while the second one is very much damped (decay rate of 1386 1/s) and its frequency is not much affected by the spin speed up to above 1000 rad/s. Also the translational mode is always damped in the whole speed range considered.

The results of a numerical simulation performed using the non-linear, the semi-linearized and the fully linearized models are reported in Figure 4. All initial generalized displacements and velocities are equal to zero, except for $\varphi_{y_1} = 0{\cdot}12$ rad; $\varphi_{y_2} = 0{\cdot}08$ rad; $\dot{\varphi}_{X_1} = \dot{\varphi}_{X_2} = -145$ rad/s; $\dot{\theta}_1 = \dot{\theta}_2 = 1000$ rad/s. Note that the displacements remain vanishingly small as the coupling terms of the damping matrix depend linearily on the displacements and hence the initial conditions assumed make them remain equal to zero for the whole integration time. The result is a whirling motion with a peak to peak amplitude of about 0·2 rad (more than 10°) in which the two bodies move together, after a short transient in which the oscillations of one relative to the other are quickly damped out. The frequency of the motion resulting from the non-linear and semi-linearized models is of 1436 and of 1450 rad/s (coinciding with that obtained from the frequency domain computation) obtained from the linearized model. The latter differ from the former by less than 1% even if the amplitude of the motion is quite large. Note the quick damping of differential motions of the two bodies while the overall whirling of the system is almost undamped; the oscillations in the angular velocity $\mathrm{d}\theta/\mathrm{d}t$ show clearly the lateral-torsional coupling, not predicted by the linearized model; such coupling is however not strong even if the amplitude is large and does not affect the lateral behaviour. Figure 4(d) shows that the energy dissipation due to the damping of the differential oscillations is large but the results of the fully non-linear solution almost coincide with those of the semi-linearized solution.

The results shown in Figure 4 support the claim that the linearized solution is still accurate in predicting the lateral behaviour even at amplitudes as large as 10° (peak to peak) and that the torsional-lateral coupling is not too strong.

Case 2 deals with a rotor having the same inertial properties of the previous one, but with a very soft connection. The translational mode is a supercritical one (i.e., the corresponding whirl speed is smaller than the spin speed or, in other words, the spin speed is higher than the critical speed related to the translational mode) and

TABLE 2

Data for the four cases studied through numerical integration. $K = 2k + 4k_t$, $C = 2c + 4c_t$, $\chi = 2(ka^2 + k_t b^2)$ *and* $\Gamma = 2(ca^2 + c_t b^2)$ *are the stiffness and damping coefficients for linearized flexural translations and rotations*

Case n.	m [kg]	J_p [kg m^2]	J_t [kg m^2]	$a = b$ [m]	$k = k_t$ [N/m]	c [Ns/m]	c_t [Ns/m]	K [N/m]	C [Ns/m]	χ [Nm/rad]	Γ [Nms/rad]
1	20 20	0·015 0·014	0·010 0·010	0·25	4×10^6	45·1	68	24×10^6	362·2	1×10^6	14·14
2	20 20	0·015 0·014	0·010 0·010	0·25	2000	1·01	1·52	12 000	8·1	500	0·316
3	20 20	0·010 0·010	0·015 0·014	0·25	4×10^6	79·5	56·6	24×10^6	385·6	1×10^6	17·02
4	20 20	0·010 0·010	0·015 0·014	0·25	4000	2·51	1·79	24 000	13·6	1000	0·538

TABLE 3

Results for the linearized analysis of the four free rotors described in Table 2; *translational modes. The flexural and torsional natural frequencies* λ_n (*which are themselves coincident*) *coincide with the critical speed* ω_{cr} *of the undamped system, owing to the decoupling between translational and rotational modes. The complex eigenfrequencies at standstill* ($\lambda(\omega = 0)$) *and the complex whirl speed at a spin speed of* 1000 *rad/s for backward and forward whirling* $\lambda_B(\omega = 1000)$, $\lambda_F(\omega = 1000)$ *are also reported. Only the values different from zero are reported*

Case n.	$\lambda_n = \omega_{cr}$ [rad/s]	$\lambda(\omega = 0)$ [rad/s]	$\lambda_B(\omega = 1000)$ [rad/s]	$\lambda_F(\omega = 1000)$ [rad/s]
1	1550	1549 + 18.1i	1549 + 29·8i	1549 + 6·4i
2	34·64	34·64 + 0·41i	36·38 + 11·5i	36·38 − 10·7i
3	1550	1549 + 19·13i	1549 + 31·7i	1549 + 6·8i
4	48·99	48·99 + 0·68i	50·78 + 14·1i	50·78 − 12·7i

the linearized analysis shows that it is unstable. Owing to the uncoupling, the rotational modes are however subcritical as there is no critical speed linked to rotational degrees of freedom.

The linearized results at 1000 rad/s show that the rigid-body precessional motion occurs at 1425 rad/s (i.e., at a frequency slightly lower than $\omega J_p/J_t$) and is strongly coupled to the forward mode involving relative motions of the two parts of the system, which occurs at 1541 rad/s. As a result, both modes are very strongly damped, with decay rates of the order of 4 and 17 1/s. The presence of the damper between the two bodies causes not only the differential motions to die out quickly, but also the overall whirling to decay. The results of a numerical simulation performed using the non-linear, the semi-linearized and the fully linearized models are reported in Figure 5. The initial conditions are the same as in the previous example, except for $\dot{\varphi}_{X_1} = \dot{\varphi}_{X_2} = -142{\cdot}5$ rad/s. The result is a decaying whirling motion with an initial peak to peak amplitude of about 0·2 rad (more than 10°). Note that the instability of the translational mode would, in an actual case, drive to instability also the rotational one; this effect is not accounted for in the simulation owing to the initial displacements and velocities which have been assumed to be exactly equal to zero.

The time history of angles φ_{X_i} and φ_{y_i} shows that a sort of beat is present, owing to the fact that two natural frequencies are quite close. The overall motion is damped. Figure 5(c), related to the spin speed of the rotor $d\theta_i/dt$, shows that a lateral-torsional coupling, not predicted by the linearized model, is again present but is not very strong even if the amplitude is large and does not affect the lateral behaviour. The plot of the time history of the total and kinetic energy shows that the fully non-linear solution gives results which are quite different from the semi-linearized solution; the difference between the two is however magnified by the very expanded scale and the relative error is still quite small. Except for this last result, the fully non-linear solution is completely superimposed on the

TABLE 4

Results for the linearized analysis of the four free rotors described in Table 2; *rotational modes. The flexural and torsional natural frequencies* λ_n *and* λ_{n_t} *and the critical speed* ω_{cr} *of the undamped system are reported together with the complex eigenfrequencies at standstill* ($\lambda(\omega = 0)$) *and the complex whirl speed at a spin speed of* 1000 *rad/s for backward and forward whirling* $\lambda_B(\omega = 1000)$, $\lambda_{F_1}(\omega = 1000)$ *and* $\lambda_{F_2}(\omega = 1000)$. *Only the values different from zero are reported*

Case n.	λ_n [rad/s]	λ_{n_t} [rad/s]	ω_{cr} [rad/s]	$\lambda(\omega = 0)$ [rad/s]	$\lambda_B(\omega = 1000)$ [rad/s]	$\lambda_{F_1}(\omega = 1000)$ [rad/s]	$\lambda_{F_2}(\omega = 1000)$ [rad/s]
1	14 140	11 751	—	14 071 + 1414i	13 360 + 1442i	$1450 + 1{\cdot}15 \times 10^{-8}$i	14 815 + 1 386i
2	316	263	—	315 + 31·6i	65·5 + 42·6i	1425 + 3·9i	1541 + 16·6i
3	11 751	14 140	21 213	11 692 + 1 175i	11 352 + 1 241i	$690 - 1{\cdot}49 \times 10^{-9}$i	12 043 + 1 109i
4	372	447	671	369·8 + 37·2i	163 + 85i	687 − 0·44i	857 − 10·3i

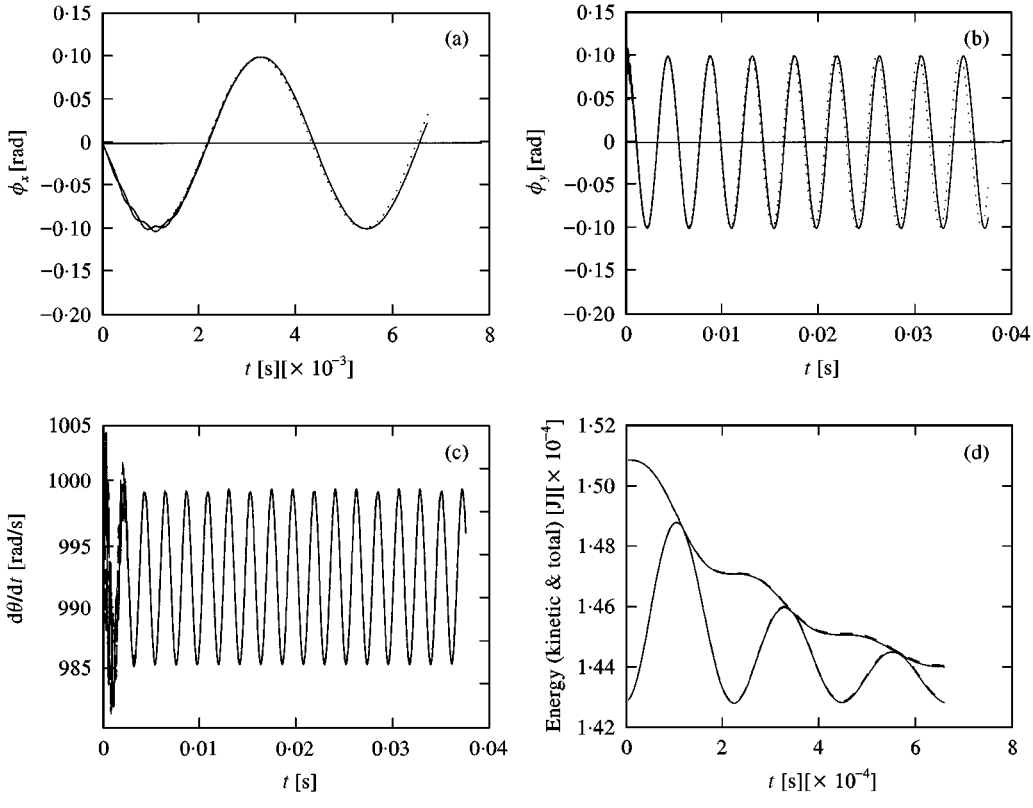

Figure 4. Twin-rigid-bodies rotor; results of the numerical simulation for case 1. Time history of (a) angles φ_{X_i}; (b) angles φ_{y_i}; (c) spin speed of the two rotors $d\theta_i/dt$ and (d) total and kinetic energy. —— non-linear, – – – semi-linear, ···· linear (only in a and b). The plots are related to different time intervals.

semi-linearized solution and the linearized model yields similar results, but overestimates the frequency by about 1%.

To investigate the discrepancies between the time history of the total and kinetic energy computed using the non-linear and semi-linearized solutions the simulation has been repeated with initial conditions on the displacements and velocities (except the spin speed) divided by 10 (Figure 6). The peak-to-peak amplitude is now of about 1° and the results of the two models are very close to each other.

Cases 3 and 4 deal with rotors with a polar moment of inertia smaller than the transversal one (long rotors). In this case two critical speeds are present, one linked to the rotational and one to the translational mode. The rotor of case 3 has a very stiff connection between the bodies and operates at the nominal speed (1000 rad/s) in the subcritical regime, while that of case 4, whose springs are far softer, at the same speed operates in supercritical conditions for both modes. The linearized analysis shows that the former is very weakly unstable in the small: the imaginary part of the whirl speed of the first forward mode is negative, but its absolute value is so small ($1{\cdot}49 \times 10^{-9}$ 1/s) that a very long time is expected to be needed to develop an actual unstable behaviour. This type of behaviour is typical of all free rotors in which $J_p < J_t$.

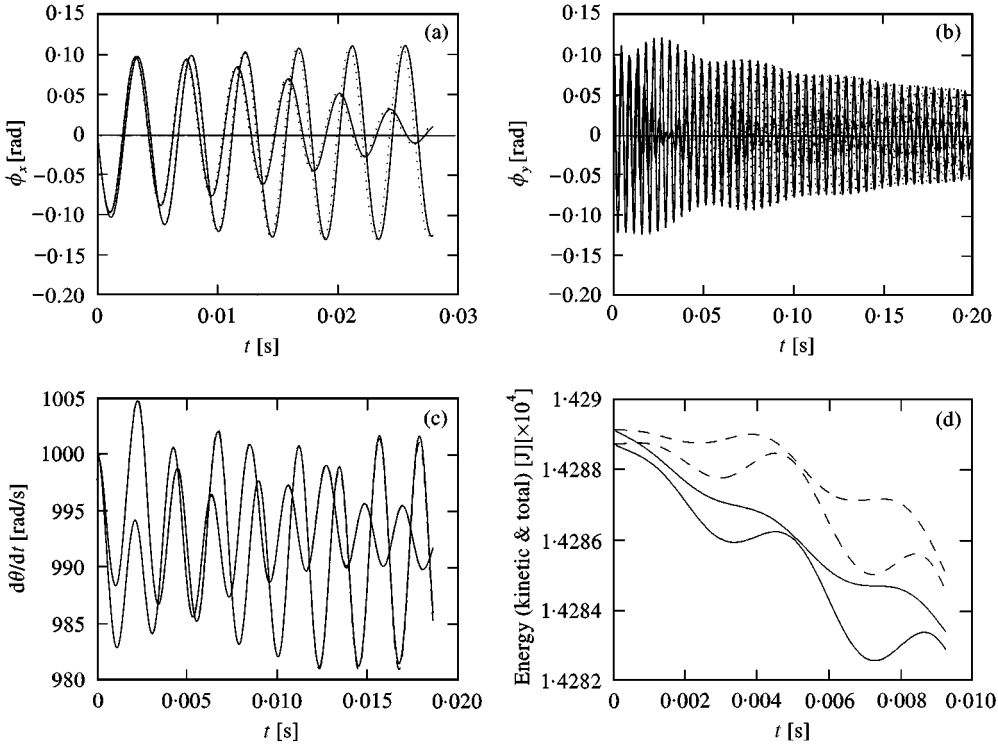

Figure 5. Same as Figure 4, but for case 2.

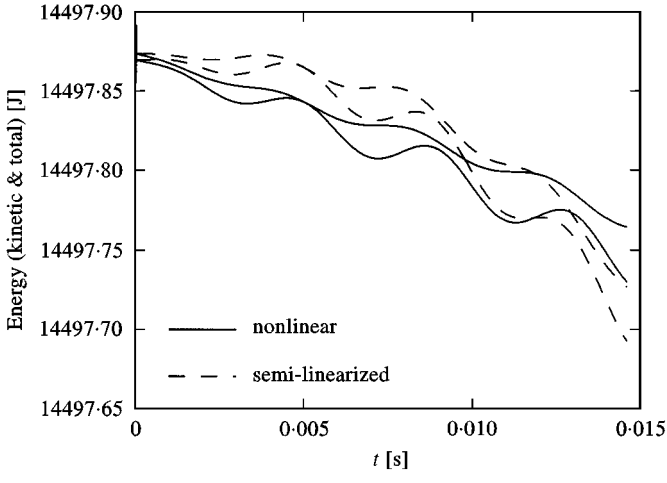

Figure 6. Same as Figure 5(d), but for an amplitude of the motion divided by 10.

The rigid-body precessional motion, occurring at 690 rad/s (i.e. at the frequency $\omega J_p/Jt$) is completely uncoupled from the mode involving relative motions of the two parts of the system. The former is slightly unstable, as said above, while the second one is very much damped and its frequency is not much affected by the spin

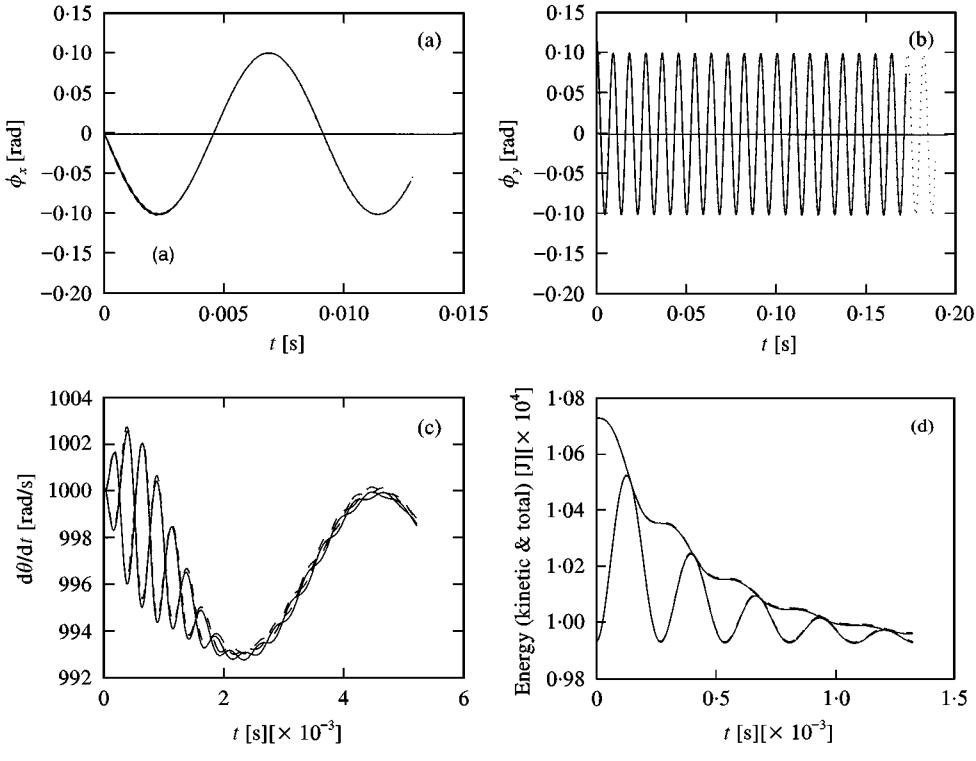

Figure 7. Same as Figure 4, but for case 3.

speed. The results of a numerical simulation performed using the non-linear, the semi-linearized and the fully linearized models are reported in Figure 7. The initial conditions are the same as for the previous cases, except for $\dot{\varphi}_{X_1} = \dot{\varphi}_{X_2} = -69$ rad/s. The result is a whirling motion with a peak to peak amplitude of about 0·2 rad (more than 10°) in which the two bodies move together, after a short transient in which the oscillations of one relative to the other are quickly damped out.

Figure 7(b) shows that the buildup of the amplitude is so slow that the time history is practically coincident with that of an undamped system. From Figure 7(d) it is clear that the time history of the total and kinetic energy computed using the fully non-linear solution is almost superimosed on the semi-linearized solution as in case 1.

The linearized analysis shows that the rotor of case 4 is very unstable in all forward modes, particularly in the translational and second rotational ones. However, also the first rotational forward mode is quite unstable, possibly owing to the closeness of the two rotational modes.

The results of a numerical simulation performed using the non-linear, the semi-linearized and the fully linearized models are reported in Figure 8. The initial conditions are the same as for case 3. The result is a whirling motion with an initial peak to peak amplitude of about 0·2 rad (more than 10°); the amplitude quickly

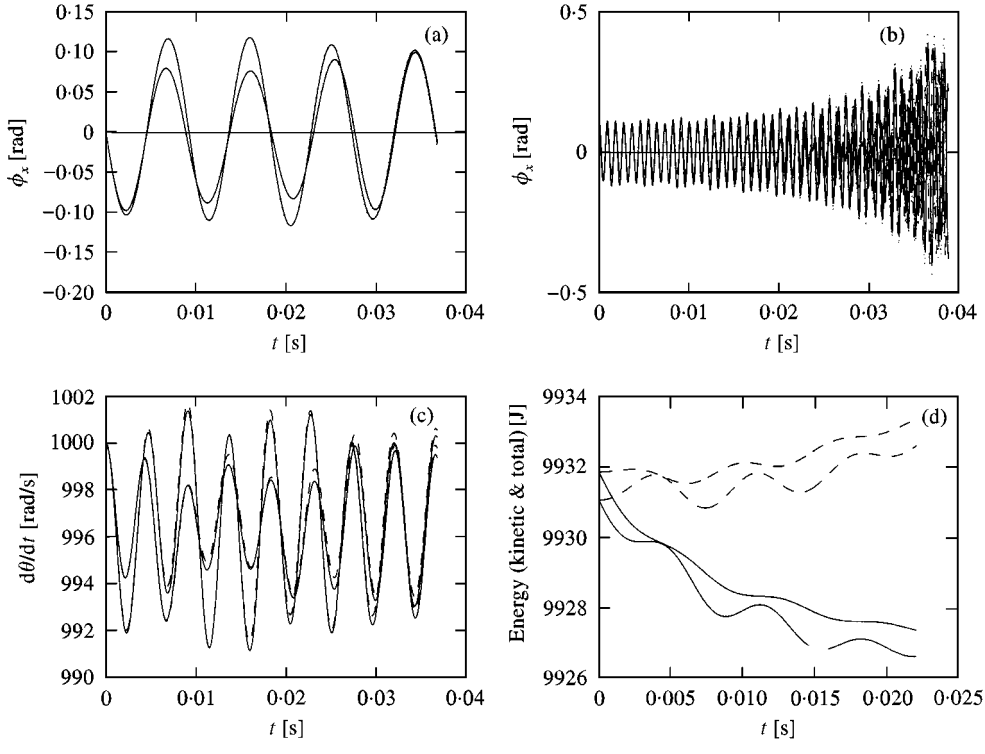

Figure 8. Same as Figure 4, but for case 4.

grows to very large values. Note that in practice the instability of the translational modes would add to that of the rotational modes owing to the coupling which would start as soon as the amplitude of the former starts to be non-negligible.

The time history of the total and kinetic energy shows that in this case, as in case 2, the non-linear solution gives results which are not in good accordance with the semi-linearized solution, but the same considerations on the smallness of the relative error still hold.

To show the effects of the non-linearities due to large amplitudes, the simulation for case 2 has been repeated with initial conditions with larger values of φ_{y_i} and $\dot{\varphi}_{X_i}$: $\varphi_{y_1} = 0{\cdot}48$ rad; $\varphi_{y_2} = 0{\cdot}32$ rad; $\dot{\varphi}_{X_1} = \dot{\varphi}_{X_2} = -570$ rad/s (Figure 9).

Owing to the very large amplitude (about 60° peak to peak), the linearized solution gives results which are quantitatively uncorrect, while being still qualitatively correct. The semi-linearized solution, is on the contrary quite reliable in predicting the behaviour of the system, except for the kinetic energy, as it was already noted in Figure 5.

4. CONCLUSIONS

A general mathematical model for multi-degrees-of-freedom rotors which does not rely on the usual assumptions of small displacements and rotations and on assumptions on the angular velocity has been obtained using the same generalized

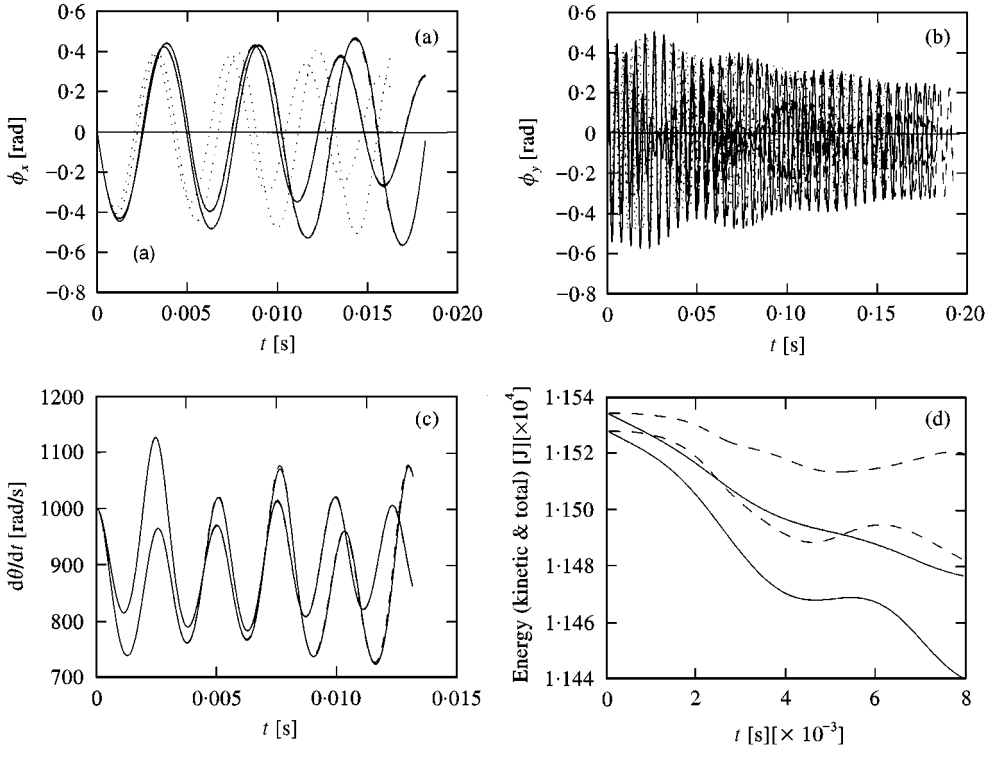

Figure 9. Same as Figure 5 (case 2), but with different initial conditions. The very large amplitude makes the linearized solution incorrect, while the semi-linearized one retains its applicability.

co-ordinates and overall approach common in rotordynamics. The model reduces to the classical formulation if the motion in the small is considered.

The formulation here described is applicable to free rotors and constitutes a bridge between classical rotordynamics and multibody spinning spacecraft dynamics, showing that, in spite of the different approach and traditional notation in the two fields, they actually deal with the same physical phenomena.

The complexity of the equations reported in Appendix A should not confuse the reader: their numerical integration is straightforward. As they deal with a non-linear problem, a closed-form solution cannot be achieved even with a different choice of the generalized co-ordinates, and the present approach has the advantage of using co-ordinates which have an immediate and intuitive physical meaning.

A number of numerical simulations have been performed, some of which are reported here, allowing one to draw the following conclusions.

- The assumption of constant angular velocity can be obtained from that of constant angular momentum, typical of free-rotor dynamics, when small amplitude motion is considered. The stability considerations drawn from classical rotordynamic analysis hold for the study of the stability in the small of free rotors and spacecrafts.
- The axial and torsional motions are coupled with the lateral behaviour of the rotor. However, this coupling becomes vanishingly small with reducing

amplitude of the latter (for the torsional motion this statement can be seen as a consequence of the previous point). The axial-flexural and torsional-flexural decoupling is then applicable to the motion in the small to both fixed and free rotors.

- The linearized analysis holds with good precision to motions occurring with angular amplitudes up to several degrees. This allows one to use the classical linearized rotordynamic approach to the study of all fixed rotors (which is fairly obvious) but also in general to free rotors, at least if they are provided with an attitude control system (which can be introduced into the model), which prevents large amplitude motions from occurring.
- In the case of multibody or discretized compliant systems, it is possible to resort to what has been here referred to as a semi-linearized model, in which the displacements of each body (generalized co-ordinates for the attitude motions) are unbounded, while the relative displacements are considered as small. Such semi-linearized model allows one to study the motion with large amplitudes of complex systems with good precision, provided that the connections between the various bodies are stiff enough to prevent large relative motions or that the amplitude of relative motions is restricted in some other way.

REFERENCES

1. S. H. Crandall 1995 (W. Kliemann and N. Sri Namachchivaya editors), *Nonlinear Dynamics and Stochastic Mechanics*. Boca Raton: CRC Press. Rotordynamics.
2. S. F. Singer 1964 *Torques and Attitude Sensing in Earth Satellites*. New York: Academic Press.
3. J. R. Wertz 1985 *Spacecraft Attitude Determination and Control* (*Written by Members of the Technical Staff Attitude Systems Operations*). Computer Sciences Corporation.
4. CNES 1986 *Mécanique spatiale pour les satellites géostationnaires*. Toulouse: CEPAD.
5. P. Hughes 1986 *Spacecraft attitude dynamics*. New York: John Wiley and Sons.
6. P. W. Fortescue and J. Stark 1991 *Spacecraft Systems Engineering*. New York: Wiley.
7. European Space Agency: http://sci.esa.int/categories/scienceprograms/.
8. University of Pisa, Space Mechanics Group: http://tycho.dm.unipi.it/nobili/ggproject.html.
9. Boeing Corporation: http://www.boeing.com/defense-space/space/spacestation/.
10. *DCAP-Dynamics and Control Analysis Package* 1993: *Reference Manual*.
11. Y. Jafry and M. Weinberger 1998 *Classical Quantum Gravity* **15**, 481–500. Evaluation of a proposed test of the weak equivalence principle using Earth-orbiting bodies in high-speed co-rotation.
12. A. Nobili *et al.* 1995 *The Journal of the Astronautical Sciences* **43**, 219–242. Galileo Galilei flight experiment on equivalence principle with field emission electric propulsion.
13. *Galileo Galilei GG* 1998: *Phase A Report*. Pisa: GG Team.
14. G. Genta and E. Brusa 1997 *Proceedings of the* 48*th International Astronautical Conference*, *Turin*, *October* 6–10. Active stabilization of a fast-spinning multibody spacecraft.
15. G. Genta and E. Brusa *International Journal of Rotating Machinery*. On the role of non synchronous rotating damping in rotordynamics. (to be published).

16. G. GENTA 1998 *Vibration of Structures and Machines*. New York: Springer, third edition.
17. G. GENTA, C. DELPRETE 1995 *Journal of Sound and Vibration* **180**, 369–386. Acceleration through critical speeds of an anisotropic, nonlinear, torsionally stiff rotor with many degrees of freedom.

APPENDIX A

A.1. REFERENCE FRAMES AND GENERALIZED CO-ORDINATES

The six generalized co-ordinates needed to describe the motion of the spinning rigid body in the tri-dimensional space can be defined with reference to the following frames (Figure 10).

- Frame OXYZ: Inertial frame. In the case of a "fixed" rotor (Figure 1), Z-axis can coincide with the rotation axis in the undeflected position and the origin O can be located in the centre of gravity of the rotor (always in the undeflected position). In the case of "free" rotors, the position and the orientation of the inertial frame is immaterial.
- Frame Gxyz with origin in the centre of gravity of the rotor G and fixed to it; z-axis coincides with the principal axis of inertia which is close, apart from the small misalignement which causes the couple unbalance, to the rotation axis of the rigid body in the deformed position and x- and y-axis are defined by the following rotations:
  — Rotate the axes of OXYZ frame about the X-axis of an angle φ_X until the Y-axis enters the rotation plane of the rigid body in its deformed configuration. Let the axes so obtained be the x*-, y*- and z*-axis. The rotation matrix allowing one to express the components of a vector in the rotated frame from those referred to the inertial frame, is

$$\mathbf{R}_1 = \begin{bmatrix} 1 & 0 & 0 \\ 0 & \cos(\varphi_X) & \sin(\varphi_X) \\ 0 & -\sin(\varphi_X) & \cos(\varphi_X) \end{bmatrix}. \tag{A1}$$

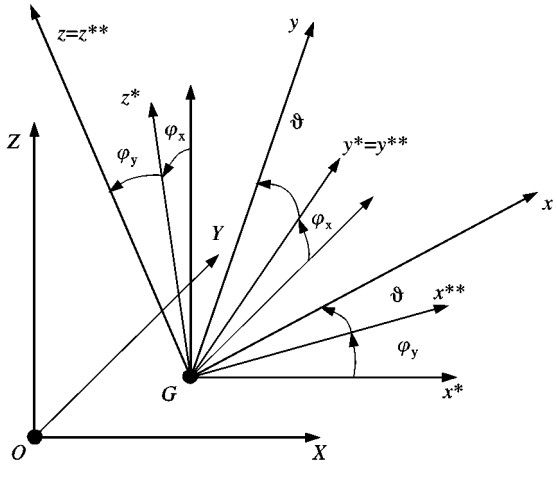

Figure 10. Reference frames.

— Rotate the G$x^*y^*z^*$ frame about the y^*-axis until the x^*-axis also enters the rotation plane of the rigid body. Let the axis so obtained be the x^{**}-axis and the rotation angle be φ_y. After the two mentioned rotations, the z^{**}-axis coincides with the symmetry axis of the rigid body in its deformed configuration. Let the matrix expressing this second rotation be

$$\mathbf{R}_2 = \begin{bmatrix} \cos(\varphi_y) & 0 & -\sin(\varphi_y) \\ 0 & 1 & 0 \\ \sin(\varphi_y) & 0 & \cos(\varphi_y) \end{bmatrix}. \tag{A2}$$

— Further rotate the G$x^{**}y^*z^{**}$ frame in the $x^{**}y^*$ plane of an angle equal to the rotation angle θ of the rotor due to the spin speed. Frame Gxyz is actually fixed to the rigid body; the matrix allowing one to express a vector in the G xyz frame from the components in the G$x^{**}y^*z$ frame is

$$\mathbf{R}_3 = \begin{bmatrix} \cos(\theta) & \sin(\theta) & 0 \\ -\sin(\theta) & \cos(\theta) & 0 \\ 0 & 0 & 1 \end{bmatrix}. \tag{A3}$$

Take the X-, Y- and Z-co-ordinates of point G and angles φ_X, φ_y, and θ as generalized co-ordinates of the rigid body.

A.1.1. *Kinetic energy and equations of motion*

To compute the kinetic energy of the rigid body, the velocity of the center of gravity (point G) and the angular velocity expressed in the principal system of inertia must be computed. The position of point G is obviously

$$(\overline{G-O}) = [X \;\; Y \;\; Z]^{\mathrm{T}}. \tag{A4}$$

The translational kinetic energy is then

$$\mathscr{T}_t = \tfrac{1}{2} m V_G^2 = \tfrac{1}{2} m(\dot{X}^2 + \dot{Y}^2 + \dot{Z}^2). \tag{A5}$$

For the computation of the rotational kinetic energy, the angular velocity must be expressed in the principal reference frame of the rotor. The three components of the angular velocity can be considered vectors acting in different directions: $\dot{\varphi}_X$ along the X-axis, $\dot{\varphi}_y$ along the y^*-axis, and $\dot{\theta}$ along the z-axis. Using the relevant rotation matrices, the components of the angular velocity along the principal axes of inertia of the rotor are

$$\boldsymbol{\Omega} = \mathbf{R}_3\mathbf{R}_2 \begin{Bmatrix} \dot{\varphi}_X \\ 0 \\ 0 \end{Bmatrix} + \mathbf{R}_3 \begin{Bmatrix} 0 \\ \dot{\varphi}_y \\ 0 \end{Bmatrix} + \begin{Bmatrix} 0 \\ 0 \\ \dot{\theta} \end{Bmatrix}. \tag{A6}$$

Without resorting to small angles assumptions, equation (A6) reduces to

$$\boldsymbol{\Omega} = \begin{Bmatrix} \dot{\varphi}_X \cos(\theta)\cos(\varphi_y) + \dot{\varphi}_y \sin(\theta) \\ -\dot{\varphi}_X \sin(\theta)\cos(\varphi_y) + \dot{\varphi}_y \cos(\theta) \\ \dot{\varphi}_X \sin(\varphi_y) + \dot{\theta} \end{Bmatrix}. \tag{A7}$$

As the components of $\boldsymbol{\Omega}$ are referred to the principal axes of inertia, the rotational kinetic energy can be easily computed as

$$\mathscr{T}_r = \tfrac{1}{2} J_x[\dot{\varphi}_X \cos(\theta)\cos(\varphi_y) + \dot{\varphi}_y \sin(\theta)]^2 + \tfrac{1}{2} J_y[-\dot{\varphi}_X \sin(\theta)\cos(\varphi_y) + \dot{\varphi}_y \cos(\theta)]^2 + \tfrac{1}{2} J_z[\dot{\varphi}_X \sin(\varphi_y) + \dot{\theta}]^2. \quad \text{(A8)}$$

The equations of motion can be obtained as usual through the Lagrange equation. The generalized forces Q_i to be included in the equations of motion will be obtained when the potential energy and the dissipation function will be defined. By performing the relevant derivatives, the six equations of motion are obtained

$$m\ddot{X} = Q_X, \qquad m\ddot{Y} = Q_Y, \qquad m\ddot{Z} = Q_Z, \quad \text{(A9)}$$

$$\begin{aligned}
&\{[J_x \cos^2(\theta) + J_y \sin^2(\theta)]\cos^2(\varphi_y) + J_z \sin^2(\varphi_y)\}\ddot{\varphi}_X + (J_x - J_y)\sin(\theta)\cos(\theta)\cos(\varphi_y)\ddot{\varphi}_y \\
&\quad + J_p \sin(\varphi_y)\ddot{\theta} - 2(J_x - J_y)\sin(\theta)\cos(\theta)\cos^2(\varphi_y)\dot{\theta}\dot{\varphi}_X \\
&\quad + \{(J_x - J_y)[\cos^2(\theta) - \sin^2(\theta)] + J_z\} \\
&\quad \times \cos(\varphi_y)\dot{\theta}\dot{\varphi}_y - 2\{[J_x \cos(^2(\theta) + J_y \sin^2(\theta)] - J_z\}\cos(\varphi_y)\sin(\varphi_y)\dot{\varphi}_X\dot{\varphi}_y \\
&\quad - (J_x - J_y)\sin(\theta)\cos(\theta)\sin(\varphi_y)\dot{\varphi}_y^2 = Q_{\varphi_X}, \\
&[J_x \sin^2(\theta) + J_y \cos^2(\theta)]\ddot{\varphi}_y + (J_x - J_y)\sin(\theta)\cos(\theta)\cos(\varphi_y)\ddot{\varphi}_X \\
&\quad + 2(J_x - J_y)\sin(\theta)\cos(\theta)\dot{\theta}\dot{\varphi}_y \\
&\quad + \{(J_x - J_y)[\cos^2(\theta) - \sin^2(\theta)] - J_z\}\cos(\varphi_y)\dot{\theta}\dot{\varphi}_X + [J_x \cos^2(\theta) + J_y \sin^2(\theta) - J_z] \\
&\quad \times \cos(\varphi_y)\sin(\varphi_y)\dot{\varphi}_X^2 = Q_{\varphi_y}, \\
&J_p\ddot{\theta} + J_p \sin(\varphi_y)\ddot{\varphi}_X - \{(J_x - J_y)[\cos^2(\theta) - \sin^2(\theta)] - J_z\}\cos(\varphi_y)\dot{\varphi}_y\dot{\varphi}_X \\
&\quad + (J_x - J_y)\sin(\theta)\cos(\theta)\cos^2(\varphi_y)\dot{\varphi}_X^2 - (J_x - J_y)\sin(\theta)\cos(\theta)\dot{\varphi}_y^2 = Q_\theta.
\end{aligned} \quad \text{(A10)}$$

A.2. POTENTIAL ENERGY AND GENERALIZED FORCES

Consider two rigid bodies, referred to as body 1 and body 2, connected by a linear spring (Figure 3). Let the end point of the spring connected with body 1 (point P_1) have co-ordinates $x_1 y_1 z_1$ in the reference frame fixed to the latter and the other end point (point P_2) have co-ordinates $x_2 y_2 z_2$ in the reference frame fixed to the other body. Their co-ordinates in the inertial frame are

$$(\overline{P_i - O}) = \mathbf{R}_{1_i}^{\mathrm{T}} \mathbf{R}_{2_i}^{\mathrm{T}} \mathbf{R}_{3_i}^{\mathrm{T}} \begin{Bmatrix} x_i \\ y_i \\ z_i \end{Bmatrix} + \begin{Bmatrix} X_i \\ Y_i \\ Z_i \end{Bmatrix}, \quad \text{(A11)}$$

for $i = 1, 2$.

The potential energy stored in the spring of stiffness k is

$$\mathscr{U} = \tfrac{1}{2}\, k[(\overline{P_1 - O}) - (\overline{P_2 - O})]^{\mathrm{T}}\,[(\overline{P_1 - O}) - (\overline{P_2 - O})]. \tag{A12}$$

Equation (A12) can be expanded to

$$\begin{aligned}
\mathscr{U} = \tfrac{1}{2}\, k\Big(& (X_1 - X_2)^2 + (Y_1 - Y_2)^2 + (Z_1 - Z_2)^2 + x_1^2 + y_1^2 + z_1^2 + x_2^2 + y_2^2 + z_2^2 \\
& + 2(X_1 - X_2)[\cos(\theta_1)\cos(\varphi_{y_1})x_1 - \sin(\theta_1)\cos(\varphi_{y_1})y_1 + \sin(\varphi_{y_1})z_1 \\
& - \cos(\theta_2)\cos(\varphi_{y_2})x_2 + \sin(\theta_2)\cos(\varphi_{y_2})y_2 - \sin(\varphi_{y_2})z_2] \\
& + 2(Y_1 - Y_2)[\cos(\theta_1)\sin(\varphi_{y_1})\sin(\varphi_{x_1})x_1 + \sin(\theta_1)\cos(\varphi_{x_1})x_1 \\
& - \sin(\theta_1)\sin(\varphi_{y_1})\sin(\varphi_{x_1})y_1 + \cos(\theta_1)\cos(\varphi_{x_1})y_1 - \cos(\varphi_{y_1})\sin(\varphi_{x_1})z_1 \\
& - \cos(\theta_2)\sin(\varphi_{y_2})\sin(\varphi_{x_2})x_2 - \sin(\theta_2)\cos(\varphi_{x_2})x_2 + \sin(\theta_2)\sin(\varphi_{y_2})\sin(\varphi_{x_2})y_2 \\
& - \cos(\theta_2)\cos(\varphi_{x_2})y_2 + \cos(\varphi_{y_2})\sin(\varphi_{x_2})z_2] \\
& + 2(Z_1 - Z_2)[- \cos(\theta_1)\sin(\varphi_{y_1})\cos(\varphi_{x_1})x_1 \\
& + \sin(\theta_1)\sin(\varphi_{x_1})x_1 + \sin(\theta_1)\sin(\varphi_{y_1})\cos(\varphi_{x_1})y_1 + \cos(\theta_1)\sin(\varphi_{x_1})y_1 \\
& + \cos(\varphi_{y_1})\cos(\varphi_{x_1})z_1 + \cos(\theta_2)\sin(\varphi_{y_2})\cos(\varphi_{x_2})x_2 - \sin(\theta_2)\sin(\varphi_{x_2})x_2 \\
& - \sin(\theta_2)\sin(\varphi_{y_2})\cos(\varphi_{x_2})y_2 - \cos(\theta_2)\sin(\varphi_{x_2})y_2 - \cos(\varphi_{y_2})\cos(\varphi_{x_2})z_2] \\
& + 2\{ - \cos(\theta_1)\cos(\theta_2)[\sin(\varphi_{y_1})\sin(\varphi_{y_2})\cos(\varphi_{x_2} - \varphi_{x_1}) + \cos(\varphi_{y_1})\cos(\varphi_{y_2})] \\
& + [\cos(\theta_1)\sin(\theta_2)\sin(\varphi_{y_1}) - \sin(\theta_1)\cos(\theta_2)\sin(\varphi_{y_2})]\sin(\varphi_{x_2} - \varphi_{x_1}) \\
& - \sin(\theta_1)\sin(\theta_2)\cos(\varphi_{x_2} - \varphi_{x_1})\}x_1x_2 \\
& + 2\{\cos(\theta_1)\sin(\theta_2)[\sin(\varphi_{y_1})\sin(\varphi_{y_2})\cos(\varphi_{x_2} - \varphi_{x_1}) + \cos(\varphi_{y_1})\cos(\varphi_{y_2})] \\
& + [\cos(\theta_1)\cos(\theta_2)\sin(\varphi_{y_1}) + \sin(\theta_1)\sin(\theta_2)\sin(\varphi_{y_2})]\sin(\varphi_{x_2} - \varphi_{x_1}) \\
& - \sin(\theta_1)\cos(\theta_2)\cos(\varphi_{x_2} - \varphi_{x_1})\}x_1y_2 \\
& + 2[\cos(\theta_1)\sin(\varphi_{y_1})\cos(\varphi_{y_2})\cos(\varphi_{x_2} - \varphi_{x_1}) + \sin(\theta_1)\cos(\varphi_{y_2})\sin(\varphi_{x_2} - \varphi_{x_1}) \\
& - \cos(\theta_1)\cos(\varphi_{y_1})\sin(\varphi_{y_2})]x_1z_2 + 2\{\sin(\theta_1)\cos(\theta_2)[\sin(\varphi_{y_1})\sin(\varphi_{y_2})\cos(\varphi_{x_2} - \varphi_{x_1}) \\
& + \cos(\varphi_{y_1})\cos(\varphi_{y_2})] - [\sin(\theta_1)\sin(\theta_2)\sin(\varphi_{y_1}) \\
& + \cos(\theta_1)\cos(\theta_2)\sin(\varphi_{y_2})]\sin(\varphi_{x_2} - \varphi_{x_1}) - \cos(\theta_1)\sin(\theta_2)\cos(\varphi_{x_2} - \varphi_{x_1})\}y_1x_2 \\
& + 2\{ - \sin(\theta_1)\sin(\theta_2)[\sin(\varphi_{y_1})\sin(\varphi_{y_2})\cos(\varphi_{x_2} - \varphi_{x_1}) + \cos(\varphi_{y_1})\cos(\varphi_{y_2})] \\
& + [\cos(\theta_1)\sin(\theta_2)\sin(\varphi_{y_2}) - \sin(\theta_1)\cos(\theta_2)\sin(\varphi_{y_1})]\sin(\varphi_{x_2} - \varphi_{x_1}) \\
& - \cos(\theta_1)\cos(\theta_2)\cos(\varphi_{x_2} - \varphi_{x_1})\}y_1y_2 \\
& + 2[- \sin(\theta_1)\sin(\varphi_{y_1})\cos(\varphi_{y_2})\cos(\varphi_{x_2} - \varphi_{x_1}) + \cos(\theta_1)\cos(\varphi_{y_2})\sin(\varphi_{x_2} - \varphi_{x_1})
\end{aligned}$$

$$+ \sin(\theta_1)\cos(\varphi_{y_1})\sin(\varphi_{y_2})]y_1z_2 + 2[\cos(\theta_2)\cos(\varphi_{y_1})\sin(\varphi_{y_2})\cos(\varphi_{x_2} - \varphi_{x_1})$$
$$- \sin(\theta_2)\cos(\varphi_{y_1})\sin(\varphi_{x_2} - \varphi_{x_1}) - \cos(\theta_2)\sin(\varphi_{y_1})\cos(\varphi_{y_2})]z_1x_2$$
$$+ 2[-\sin(\theta_2)\cos(\varphi_{y_1})\sin(\varphi_{y_2})\cos(\varphi_{x_2}-\varphi_{x_1})-\cos(\theta_2)\cos(\varphi_{y_1})\sin(\varphi_{x_2}-\varphi_{x_1})$$
$$+ \sin(\theta_2)\sin(\varphi_{y_1})\cos(\varphi_{y_2})]z_1y_2 + 2[-\cos(\varphi_{y_1})\cos(\varphi_{y_2})\cos(\varphi_{x_2} - \varphi_{x_1})$$
$$- \sin(\varphi_{y_1})\sin(\varphi_{y_2})]z_1z_2\Big). \tag{A13}$$

The generalized forces can then be obtained:

$$Q_{X_1} = -\frac{\partial \mathscr{U}}{\partial X_1} = -k[X_1 - X_2 + \cos(\theta_1)\cos(\varphi_{y_1})x_1 - \sin(\theta_1)\cos(\varphi_{y_1})y_1$$
$$+ \sin(\varphi_{y_1})z_1 - \cos(\theta_2)\cos(\varphi_{y_2})x_2 + \sin(\theta_2)\cos(\varphi_{y_2})y_2 - \sin(\varphi_{y_2})z_2], \tag{A14}$$

$$Q_{Y_1} = -\frac{\partial \mathscr{U}}{\partial Y_1} = -k[Y_1 - Y_2 + \cos(\theta_1)\sin(\varphi_{y_1})\sin(\varphi_{x_1})x_1 + \sin(\theta_1)\cos(\varphi_{x_1})x_1$$
$$- \sin(\theta_1)\sin(\varphi_{y_1})\sin(\varphi_{x_1})y_1 + \cos(\theta_1)\cos(\varphi_{x_1})y_1 - \cos(\varphi_{y_1})\sin(\varphi_{x_1})z_1$$
$$-\cos(\theta_2)\sin(\varphi_{y_2})\sin(\varphi_{x_2})x_2-\sin(\theta_2)\cos(\varphi_{x_2})x_2+\sin(\theta_2)\sin(\varphi_{y_2})\sin(\varphi_{x_2})y_2$$
$$- \cos(\theta_2)\cos(\varphi_{x_2})y_2 + \cos(\varphi_{y_2})\sin(\varphi_{x_2})z_2], \tag{A15}$$

$$Q_{Z_1} = -\frac{\partial \mathscr{U}}{\partial Z_1} = -k[Z_1 - Z_2 - \cos(\theta_1)\sin(\varphi_{y_1})\cos(\varphi_{x_1})x_1 + \sin(\theta_1)\sin(\varphi_{x_1})x_1$$
$$+ \sin(\theta_1)\sin(\varphi_{y_1})\cos(\varphi_{x_1})y_1 + \cos(\theta_1)\sin(\varphi_{x_1})y_1 + \cos(\varphi_{y_1})\cos(\varphi_{x_1})z_1$$
$$+ \cos(\theta_2)\sin(\varphi_{y_2})\cos(\varphi_{x_2})x_2 - \sin(\theta_2)\sin(\varphi_{x_2})x_2$$
$$- \sin(\theta_2)\sin(\varphi_{y_2})\cos(\varphi_{x_2})y_2 - \cos(\theta_2)\sin(\varphi_{x_2})y_2 - \cos(\varphi_{y_2})\cos(\varphi_{x_2})z_2], \tag{A16}$$

$$Q_{\varphi_{X_1}} = -\frac{\partial \mathscr{U}}{\partial \phi_{X_1}} = -k\Big((Y_1 - Y_2)[\cos(\theta_1)\sin(\varphi_{y_1})\cos(\varphi_{x_1})x_1 - \sin(\theta_1)\sin(\varphi_{x_1})x_1$$
$$- \sin(\theta_1)\sin(\varphi_{y_1})\cos(\varphi_{x_1})y_1 - \cos(\theta_1)\sin(\varphi_{x_1})y_1 - \cos(\varphi_{y_1})\cos(\varphi_{x_1})z_1]$$
$$+ (Z_1 - Z_2)[\cos(\theta_1)\sin(\varphi_{y_1})\sin(\varphi_{x_1})x_1 + \sin(\theta_1)\cos(\varphi_{x_1})x_1$$
$$- \sin(\theta_1)\sin(\varphi_{y_1})\sin(\varphi_{x_1})y_1 + \cos(\theta_1)\cos(\varphi_{x_1})y_1 - \cos(\varphi_{y_1})\sin(\varphi_{x_1})z_1]$$
$$+ \{-\cos(\theta_1)\cos(\theta_2)\sin(\varphi_{y_1})\sin(\varphi_{y_2})\sin(\varphi_{x_2} - \varphi_{x_1})$$
$$- [\cos(\theta_1)\sin(\theta_2)\sin(\varphi_{y_1}) - \sin(\theta_1)\cos(\theta_2)\sin(\varphi_{y_2})]\cos(\varphi_{x_2} - \varphi_{x_1})$$
$$- \sin(\theta_1)\sin(\theta_2)\sin(\varphi_{x_2} - \varphi_{x_1})\}x_1x_2$$

$$
\begin{aligned}
&+\{\cos(\theta_1)\sin(\theta_2)\sin(\varphi_{y_1})\sin(\varphi_{y_2})\sin(\varphi_{x_2}-\varphi_{x_1})-[\cos(\theta_1)\cos(\theta_2)\sin(\varphi_{y_1})\\
&+\sin(\theta_1)\sin(\theta_2)\sin(\varphi_{y_2})]\cos(\varphi_{x_2}-\varphi_{x_1})-\sin(\theta_1)\cos(\theta_2)\sin(\varphi_{x_2}-\varphi_{x_1})\}x_1y_2\\
&+[\cos(\theta_1)\sin(\varphi_{y_1})\cos(\varphi_{y_2})\sin(\varphi_{x_2}-\varphi_{x_1})-\sin(\theta_1)\cos(\varphi_{y_2})\cos(\varphi_{x_2}-\varphi_{x_1})]x_1z_2\\
&+\{\sin(\theta_1)\cos(\theta_2)\sin(\varphi_{y_1})\sin(\varphi_{y_2})\sin(\varphi_{x_2}-\varphi_{x_1})+[\sin(\theta_1)\sin(\theta_2)\sin(\varphi_{y_1})\\
&+\cos(\theta_1)\cos(\theta_2)\sin(\varphi_{y_2})]\cos(\varphi_{x_2}-\varphi_{x_1})-\cos(\theta_1)\sin(\theta_2)\sin(\varphi_{x_2}-\varphi_{x_1})\}y_1x_2\\
&+\{-\sin(\theta_1)\sin(\theta_2)\sin(\varphi_{y_1})\sin(\varphi_{y_2})\sin(\varphi_{x_2}-\varphi_{x_1})-[\cos(\theta_1)\sin(\theta_2)\sin(\varphi_{y_2})\\
&-\sin(\theta_1)\cos(\theta_2)\sin(\varphi_{y_1})]\cos(\varphi_{x_2}-\varphi_{x_1})-\cos(\theta_1)\cos(\theta_2)\sin(\varphi_{x_2}-\varphi_{x_1})\}y_1y_2\\
&+[-\sin(\theta_1)\sin(\varphi_{y_1})\cos(\varphi_{y_2})\sin(\varphi_{x_2}-\varphi_{x_1})\\
&-\cos(\theta_1)\cos(\varphi_{y_2})\cos(\varphi_{x_2}-\varphi_{x_1})]y_1z_2\\
&+[\cos(\theta_2)\cos(\varphi_{y_1})\sin(\varphi_{y_2})\sin(\varphi_{x_2}-\varphi_{x_1})\\
&+\sin(\theta_2)\cos(\varphi_{y_1})\cos(\varphi_{x_2}-\varphi_{x_1})]z_1x_2\\
&+[-\sin(\theta_2)\cos(\varphi_{y_1})\sin(\varphi_{y_2})\sin(\varphi_{x_2}-\varphi_{x_1})\\
&+\cos(\theta_2)\cos(\varphi_{y_1})\cos(\varphi_{x_2}-\varphi_{x_1})]z_1y_2\\
&-\cos(\varphi_{y_1})\cos(\varphi_{y_2})\sin(\varphi_{x_2}-\varphi_{x_1})z_1z_2\Big)
\end{aligned}
\tag{A17}
$$

$$
\begin{aligned}
Q_{\varphi_{y_1}}=-\frac{\partial \mathscr{U}}{\partial \phi_{y_1}}=-k\Big(&(X_1-X_2)[-\cos(\theta_1)\sin(\varphi_{y_1})x_1+\sin(\theta_1)\sin(\varphi_{y_1})y_1+\cos(\varphi_{y_1})z_1]\\
&+(Y_1-Y_2)[\cos(\theta_1)\cos(\varphi_{y_1})\sin(\varphi_{x_1})x_1-\sin(\theta_1)\cos(\varphi_{y_1})\sin(\varphi_{x_1})y_1\\
&+\sin(\varphi_{y_1})\sin(\varphi_{x_1})z_1]+(Z_1-Z_2)[-\cos(\theta_1)\cos(\varphi_{y_1})\cos(\varphi_{x_1})x_1\\
&+\sin(\theta_1)\cos(\varphi_{y_1})\cos(\varphi_{x_1})y_1-\sin(\varphi_{y_1})\cos(\varphi_{x_1})z_1]\\
&+\{-\cos(\theta_1)\cos(\theta_2)[\cos(\varphi_{y_1})\sin(\varphi_{y_2})\cos(\varphi_{x_2}-\varphi_{x_1})\\
&-\sin(\varphi_{y_1})\cos(\varphi_{y_2})]+\cos(\theta_1)\sin(\theta_2)\cos(\varphi_{y_1})\sin(\varphi_{x_2}-\varphi_{x_1})\}x_1x_2\\
&+\{\cos(\theta_1)\sin(\theta_2)[\cos(\varphi_{y_1})\sin(\varphi_{y_2})\cos(\varphi_{x_2}-\varphi_{x_1})-\sin(\varphi_{y_1})\cos(\varphi_{y_2})]\\
&+\cos(\theta_1)\cos(\theta_2)\cos(\varphi_{y_1})\sin(\varphi_{x_2}-\varphi_{x_1})\}x_1y_2\\
&+[\cos(\theta_1)\cos(\varphi_{y_1})\cos(\varphi_{y_2})\cos(\varphi_{x_2}-\varphi_{x_1})+\cos(\theta_1)\sin(\varphi_{y_1})\sin(\varphi_{y_2})]x_1z_2\\
&+\{\sin(\theta_1)\cos(\theta_2)[\cos(\varphi_{y_1})\sin(\varphi_{y_2})\cos(\varphi_{x_2}-\varphi_{x_1})-\sin(\varphi_{y_1})\cos(\varphi_{y_2})]\\
&-\sin(\theta_1)\sin(\theta_2)\cos(\varphi_{y_1})\sin(\varphi_{x_2}-\varphi_{x_1})\}y_1x_2\\
&+\{-\sin(\theta_1)\sin(\theta_2)[\cos(\varphi_{y_1})\sin(\varphi_{y_2})\cos(\varphi_{x_2}-\varphi_{x_1})-\sin(\varphi_{y_1})\cos(\varphi_{y_2})]\\
&-\sin(\theta_1)\cos(\theta_2)\cos(\varphi_{y_1})\sin(\varphi_{x_2}-\varphi_{x_1})\}y_1y_2
\end{aligned}
$$

$$
\begin{aligned}
&- [\sin(\theta_1)\cos(\varphi_{y_1})\cos(\varphi_{y_2})\cos(\varphi_{x_2} - \varphi_{x_1}) + \sin(\theta_1)\sin(\varphi_{y_1})\sin(\varphi_{y_2})]y_1z_2 \\
&+ [-\cos(\theta_2)\sin(\varphi_{y_1})\sin(\varphi_{y_2})\cos(\varphi_{x_2} - \varphi_{x_1}) + \sin(\theta_2)\sin(\varphi_{y_1})\sin(\varphi_{x_2} - \varphi_{x_1}) \\
&- \cos(\theta_2)\cos(\varphi_{y_1})\cos(\varphi_{y_2})]z_1x_2 + [\sin(\theta_2)\sin(\varphi_{y_1})\sin(\varphi_{y_2})\cos(\varphi_{x_2} - \varphi_{x_1}) \\
&+ \cos(\theta_2)\sin(\varphi_{y_1})\sin(\varphi_{x_2} - \varphi_{x_1}) + \sin(\theta_2)\cos(\varphi_{y_1})\cos(\varphi_{y_2})]z_1y_2 \\
&+ [\sin(\varphi_{y_1})\cos(\varphi_{y_2})\cos(\varphi_{x_2} - \varphi_{x_1}) - \cos(\varphi_{y_1})\sin(\varphi_{y_2})]z_1z_2\Big), \qquad \text{(A18)}
\end{aligned}
$$

$$
\begin{aligned}
Q_{\theta_1} = -\frac{\partial \mathscr{U}}{\partial \theta_1} = -k\Big(&(X_1 - X_2)[-\sin(\theta_1)\cos(\varphi_{y_1})x_1 - \cos(\theta_1)\cos(\varphi_{y_1})y_1] \\
&+ (Y_1 - Y_2)[-\sin(\theta_1)\sin(\varphi_{y_1})\sin(\varphi_{x_1})x_1 \\
&+ \cos(\theta_1)\cos(\varphi_{x_1})x_1 - \cos(\theta_1)\sin(\varphi_{y_1})\sin(\varphi_{x_1})y_1 - \sin(\theta_1)\cos(\varphi_{x_1})y_1] \\
&+ (Z_1 - Z_2)[\sin(\theta_1)\sin(\varphi_{y_1})\cos(\varphi_{x_1})x_1 + \cos(\theta_1)\sin(\varphi_{x_1})x_1 \\
&+ \cos(\theta_1)\sin(\varphi_{y_1})\cos(\varphi_{x_1})y_1 - \sin(\theta_1)\sin(\varphi_{x_1})y_1] \\
&+ \{\sin(\theta_1)\cos(\theta_2)[\sin(\varphi_{y_1})\sin(\varphi_{y_2})\cos(\varphi_{x_2} - \varphi_{x_1}) + \cos(\varphi_{y_1})\cos(\varphi_{y_2})] \\
&- [\sin(\theta_1)\sin(\theta_2)\sin(\varphi_{y_1}) + \cos(\theta_1)\cos(\theta_2)\sin(\varphi_{y_2})]\sin(\varphi_{x_2} - \varphi_{x_1}) \\
&- \cos(\theta_1)\sin(\theta_2)\cos(\varphi_{x_2} - \varphi_{x_1})\}x_1x_2 \\
&+ \{-\sin(\theta_1)\sin(\theta_2)[\sin(\varphi_{y_1})\sin(\varphi_{y_2})\cos(\varphi_{x_2} - \varphi_{x_1}) + \cos(\varphi_{y_1})\cos(\varphi_{y_2})] \\
&+ [-\sin(\theta_1)\cos(\theta_2)\sin(\varphi_{y_1}) + \cos(\theta_1)\sin(\theta_2)\sin(\varphi_{y_2})]\sin(\varphi_{x_2} - \varphi_{x_1}) \\
&- \cos(\theta_1)\cos(\theta_2)\cos(\varphi_{x_2} - \varphi_{x_1})\}x_1y_2 \\
&+ [-\sin(\theta_1)\sin(\varphi_{y_1})\cos(\varphi_{y_2})\cos(\varphi_{x_2} - \varphi_{x_1}) \\
&+ \cos(\theta_1)\cos(\varphi_{y_2})\sin(\varphi_{x_2} - \varphi_{x_1}) + \sin(\theta_1)\cos(\varphi_{y_1})\sin(\varphi_{y_2})]x_1z_2 \\
&+ \{\cos(\theta_1)\cos(\theta_2)[\sin(\varphi_{y_1})\sin(\varphi_{y_2})\cos(\varphi_{x_2} - \varphi_{x_1}) + \cos(\varphi_{y_1})\cos(\varphi_{y_2})] \\
&- [\cos(\theta_1)\sin(\theta_2)\sin(\varphi_{y_1}) - \sin(\theta_1)\cos(\theta_2)\sin(\varphi_{y_2})]\sin(\varphi_{x_2} - \varphi_{x_1}) \\
&+ \sin(\theta_1)\sin(\theta_2)\cos(\varphi_{x_2} - \varphi_{x_1})\}y_1x_2 \\
&+ \{-\cos(\theta_1)\sin(\theta_2)[\sin(\varphi_{y_1})\sin(\varphi_{y_2})\cos(\varphi_{x_2} - \varphi_{x_1}) \\
&+ \cos(\varphi_{y_1})\cos(\varphi_{y_2})] - [\sin(\theta_1)\sin(\theta_2)\sin(\varphi_{y_2}) \\
&+ \cos(\theta_1)\cos(\theta_2)\sin(\varphi_{y_1})]\sin(\varphi_{x_2} - \varphi_{x_1}) \\
&+ \sin(\theta_1)\cos(\theta_2)\cos(\varphi_{x_2} - \varphi_{x_1})\}y_1y_2 \\
&+ [-\cos(\theta_1)\sin(\varphi_{y_1})\cos(\varphi_{y_2})\cos(\varphi_{x_2} - \varphi_{x_1}) \\
&- \sin(\theta_1)\cos(\varphi_{y_2})\sin(\varphi_{x_2} - \varphi_{x_1}) + \cos(\theta_1)\cos(\varphi_{y_1})\sin(\varphi_{y_2})]y_1z_2\Big) \qquad \text{(A19)}
\end{aligned}
$$

$$Q_{X_2} = -Q_{X_1}, \qquad Q_{Y_2} = -Q_{Y_1}, \qquad Q_{Z_2} = -Q_{Z_1}, \tag{A20}$$

$$\begin{aligned}
Q_{\varphi_{x_1}} = -\frac{\partial \mathscr{U}}{\partial \phi_{X_2}} = -k\Big(& (Y_1 - Y_2)[-\cos(\theta_2)\sin(\varphi_{y_2})\cos(\varphi_{x_2})x_2 + \sin(\theta_2)\sin(\varphi_{x_2})x_2 \\
& + \sin(\theta_2)\sin(\varphi_{y_2})\cos(\varphi_{x_2})y_2 + \cos(\theta_2)\sin(\varphi_{x_2})y_2 + \cos(\varphi_{y_2})\cos(\varphi_{x_2})z_2] \\
& + (Z_1 - Z_2)[-\cos(\theta_2)\sin(\varphi_{y_2})\sin(\varphi_{x_2})x_2 - \sin(\theta_2)\cos(\varphi_{x_2})x_2 \\
& + \sin(\theta_2)\sin(\varphi_{y_2})\sin(\varphi_{x_2})y_2 - \cos(\theta_2)\cos(\varphi_{x_2})y_2 + \cos(\varphi_{y_2})\sin(\varphi_{x_2})z_2] \\
& + \{\cos(\theta_1)\cos(\theta_2)\sin(\varphi_{y_1})\sin(\varphi_{y_2})\sin(\varphi_{x_2} - \varphi_{x_1}) + [\cos(\theta_1)\sin(\theta_2)\sin(\varphi_{y_1}) \\
& - \sin(\theta_1)\cos(\theta_2)\sin(\varphi_{y_2})]\cos(\varphi_{x_2} - \varphi_{x_1}) + \sin(\theta_1)\sin(\theta_2)\sin(\varphi_{x_2} - \varphi_{x_1})\}x_1x_2 \\
& + \{-\cos(\theta_1)\sin(\theta_2)\sin(\varphi_{y_1})\sin(\varphi_{y_2})\sin(\varphi_{x_2} - \varphi_{x_1}) \\
& + [\cos(\theta_1)\cos(\theta_2)\sin(\varphi_{y_1}) + \sin(\theta_1)\sin(\theta_2)\sin(\varphi_{y_2})]\cos(\varphi_{x_2} - \varphi_{x_1}) \\
& + \sin(\theta_1)\cos(\theta_2)\sin(\varphi_{x_2} - \varphi_{x_1})\}x_1y_2 \\
& + [-\cos(\theta_1)\sin(\varphi_{y_1})\cos(\varphi_{y_2})\sin(\varphi_{x_2} - \varphi_{x_1}) \\
& + \sin(\theta_1)\cos(\varphi_{y_2})\cos(\varphi_{x_2} - \varphi_{x_1})]x_1z_2 \\
& + \{-\sin(\theta_1)\cos(\theta_2)\sin(\varphi_{y_1})\sin(\varphi_{y_2})\sin(\varphi_{x_2} - \varphi_{x_1}) \\
& - [\sin(\theta_1)\sin(\theta_2)\sin(\varphi_{y_1}) + \cos(\theta_1)\cos(\theta_2)\sin(\varphi_{y_2})]\cos(\varphi_{x_2} - \varphi_{x_1}) \\
& + \cos(\theta_1)\sin(\theta_2)\sin(\varphi_{x_2} - \varphi_{x_1})\}y_1x_2 \\
& + \{\sin(\theta_1)\sin(\theta_2)\sin(\varphi_{y_1})\sin(\varphi_{y_2})\sin(\varphi_{x_2} - \varphi_{x_1}) + [\cos(\theta_1)\sin(\theta_2)\sin(\varphi_{y_2}) \\
& - \sin(\theta_1)\cos(\theta_2)\sin(\varphi_{y_1})]\cos(\varphi_{x_2} - \varphi_{x_1}) + \cos(\theta_1)\cos(\theta_2)\sin(\varphi_{x_2} - \varphi_{x_1})\}y_1y_2 \\
& + [\sin(\theta_1)\sin(\varphi_{y_1})\cos(\varphi_{y_2})\sin(\varphi_{x_2} - \varphi_{x_1}) + \cos(\theta_1)\cos(\varphi_{y_2})\cos(\varphi_{x_2} - \varphi_{x_1})]y_1z_2 \\
& + [-\cos(\theta_2)\cos(\varphi_{y_1})\sin(\varphi_{y_2})\sin(\varphi_{x_2} - \varphi_{x_1}) \\
& - \sin(\theta_2)\cos(\varphi_{y_1})\cos(\varphi_{x_2} - \varphi_{x_1})]z_1x_2 \\
& + [\sin(\theta_2)\cos(\varphi_{y_1})\sin(\varphi_{y_2})\sin(\varphi_{x_2} - \varphi_{x_1}) - \cos(\theta_2)\cos(\varphi_{y_1})\cos(\varphi_{x_2} - \varphi_{x_1})]z_1y_2 \\
& + [\cos(\varphi_{y_1})\cos(\varphi_{y_2})\sin(\varphi_{x_2} - \varphi_{x_1})]z_1z_2\Big),
\end{aligned} \tag{A21}$$

$$\begin{aligned}
Q_{\varphi_{y_2}} = -\frac{\partial \mathscr{U}}{\partial \phi_{y_2}} = -k\Big(& (X_1 - X_2)[\cos(\theta_2)\sin(\varphi_{y_2})x_2 - \sin(\theta_2)\sin(\varphi_{y_2})y_2 - \cos(\varphi_{y_2})z_2] \\
& + (Y_1 - Y_2)[-\cos(\theta_2)\cos(\varphi_{y_2})\sin(\varphi_{x_2})x_2 + \sin(\theta_2)\cos(\varphi_{y_2})\sin(\varphi_{x_2})y_2 \\
& - \sin(\varphi_{y_2})\sin(\varphi_{x_2})z_2] + (Z_1 - Z_2)[\cos(\theta_2)\cos(\varphi_{y_2})\cos(\varphi_{x_2})x_2 \\
& - \sin(\theta_2)\cos(\varphi_{y_2})\cos(\varphi_{x_2})y_2 + \sin(\varphi_{y_2})\cos(\varphi_{x_2})z_2]
\end{aligned}$$

$$
\begin{aligned}
&+\{-\cos(\theta_1)\cos(\theta_2)[\sin(\varphi_{y_1})\cos(\varphi_{y_2})\cos(\varphi_{x_2}-\varphi_{x_1})-\cos(\varphi_{y_1})\sin(\varphi_{y_2})]\\
&-\sin(\theta_1)\cos(\theta_2)\cos(\varphi_{y_2})\sin(\varphi_{x_2}-\varphi_{x_1})\}x_1x_2\\
&+\{\cos(\theta_1)\sin(\theta_2)[\sin(\varphi_{y_1})\cos(\varphi_{y_2})\cos(\varphi_{x_2}-\varphi_{x_1})-\cos(\varphi_{y_1})\sin(\varphi_{y_2})]\\
&+\sin(\theta_1)\sin(\theta_2)\cos(\varphi_{y_2})\sin(\varphi_{x_2}-\varphi_{x_1})\}x_1y_2\\
&+[-\cos(\theta_1)\sin(\varphi_{y_1})\sin(\varphi_{y_2})\cos(\varphi_{x_2}-\varphi_{x_1})\\
&-\sin(\theta_1)\sin(\varphi_{y_2})\sin(\varphi_{x_2}-\varphi_{x_1})-\cos(\theta_1)\cos(\varphi_{y_1})\cos(\varphi_{y_2})]x_1z_2\\
&+\{\sin(\theta_1)\cos(\theta_2)[\sin(\varphi_{y_1})\cos(\varphi_{y_2})\cos(\varphi_{x_2}-\varphi_{x_1})-\cos(\varphi_{y_1})\sin(\varphi_{y_2})]\\
&-\cos(\theta_1)\cos(\theta_2)\cos(\varphi_{y_2})\sin(\varphi_{x_2}-\varphi_{x_1})\}y_1x_2\\
&+\{-\sin(\theta_1)\sin(\theta_2)[\sin(\varphi_{y_1})\cos(\varphi_{y_2})\cos(\varphi_{x_2}-\varphi_{x_1})-\cos(\varphi_{y_1})\sin(\varphi_{y_2})]\\
&+\cos(\theta_1)\sin(\theta_2)\cos(\varphi_{y_2})\sin(\varphi_{x_2}-\varphi_{x_1})\}y_1y_2\\
&+[\sin(\theta_1)\sin(\varphi_{y_1})\sin(\varphi_{y_2})\cos(\varphi_{x_2}-\varphi_{x_1})-\cos(\theta_1)\sin(\varphi_{y_2})\sin(\varphi_{x_2}-\varphi_{x_1})\\
&+\sin(\theta_1)\cos(\varphi_{y_1})\cos(\varphi_{y_2})]y_1z_2+[\cos(\theta_2)\cos(\varphi_{y_1})\cos(\varphi_{y_2})\cos(\varphi_{x_2}-\varphi_{x_1})\\
&+\cos(\theta_2)\sin(\varphi_{y_1})\sin(\varphi_{y_2})]z_1x_2+[-\sin(\theta_2)\cos(\varphi_{y_1})\cos(\varphi_{y_2})\cos(\varphi_{x_2}-\varphi_{x_1})\\
&-\sin(\theta_2)\sin(\varphi_{y_1})\sin(\varphi_{y_2})]z_1y_2+[\cos(\varphi_{y_1})\sin(\varphi_{y_2})\cos(\varphi_{x_2}-\varphi_{x_1})\\
&-\sin(\varphi_{y_1})\cos(\varphi_{y_2})]z_1z_2\Big) \qquad \text{(A22)}
\end{aligned}
$$

$$
\begin{aligned}
Q_{\theta_2}=-\frac{\partial \mathcal{U}}{\partial \theta_2}=-k\Big(&(X_1-X_2)[\sin(\theta_2)\cos(\varphi_{y_2})x_2+\cos(\theta_2)\cos(\varphi_{y_2})y_2]\\
&+(Y_1-Y_2)[\sin(\theta_2)\sin(\varphi_{y_2})\sin(\varphi_{x_2})x_2-\cos(\theta_2)\cos(\varphi_{x_2})x_2\\
&+\cos(\theta_2)\sin(\varphi_{y_2})\sin(\varphi_{x_2})y_2+\sin(\theta_2)\cos(\varphi_{x_2})y_2]\\
&+(Z_1-Z_2)[-\sin(\theta_2)\sin(\varphi_{y_2})\cos(\varphi_{x_2})x_2-\cos(\theta_2)\sin(\varphi_{x_2})x_2\\
&-\cos(\theta_2)\sin(\varphi_{y_2})\cos(\varphi_{x_2})y_2+\sin(\theta_2)\sin(\varphi_{x_2})y_2]\\
&+\{\cos(\theta_1)\sin(\theta_2)[\sin(\varphi_{y_1})\sin(\varphi_{y_2})\cos(\varphi_{x_2}-\varphi_{x_1})+\cos(\varphi_{y_1})\cos(\varphi_{y_2})]\\
&+[\cos(\theta_1)\cos(\theta_2)\sin(\varphi_{y_1})+\sin(\theta_1)\sin(\theta_2)\sin(\varphi_{y_2})]\sin(\varphi_{x_2}-\varphi_{x_1})\\
&-\sin(\theta_1)\cos(\theta_2)\cos(\varphi_{x_2}-\varphi_{x_1})\}x_1x_2\\
&+\{\cos(\theta_1)\cos(\theta_2)[\sin(\varphi_{y_1})\sin(\varphi_{y_2})\cos(\varphi_{x_2}-\varphi_{x_1})+\cos(\varphi_{y_1})\cos(\varphi_{y_2})]\\
&+[-\cos(\theta_1)\sin(\theta_2)\sin(\varphi_{y_1})+\sin(\theta_1)\cos(\theta_2)\sin(\varphi_{y_2})]\sin(\varphi_{x_2}-\varphi_{x_1})\\
&+\sin(\theta_1)\sin(\theta_2)\cos(\varphi_{x_2}-\varphi_{x_1})\}x_1y_2\\
&+\{-\sin(\theta_1)\sin(\theta_2)[\sin(\varphi_{y_1})\sin(\varphi_{y_2})\cos(\varphi_{x_2}-\varphi_{x_1})
\end{aligned}
$$

$$+\cos(\varphi_{y_1})\cos(\varphi_{y_2})] - [\sin(\theta_1)\cos(\theta_2)\sin(\varphi_{y_1})$$
$$-\cos(\theta_1)\sin(\theta_2)\sin(\varphi_{y_2})]\sin(\varphi_{x_2}-\varphi_{x_1})$$
$$-\cos(\theta_1)\cos(\theta_2)\cos(\varphi_{x_2}-\varphi_{x_1})\}y_1x_2$$
$$+\{-\sin(\theta_1)\cos(\theta_2)[\sin(\varphi_{y_1})\sin(\varphi_{y_2})\cos(\varphi_{x_2}-\varphi_{x_1})$$
$$+\cos(\varphi_{y_1})\cos(\varphi_{y_2})] + [\cos(\theta_1)\cos(\theta_2)\sin(\varphi_{y_2})$$
$$+\sin(\theta_1)\sin(\theta_2)\sin(\varphi_{y_1})]\sin(\varphi_{x_2}-\varphi_{x_1}) + \cos(\theta_1)\sin(\theta_2)\cos(\varphi_{x_2}-\varphi_{x_1})\}y_1y_2$$
$$+[-\sin(\theta_2)\cos(\varphi_{y_1})\sin(\varphi_{y_2})\cos(\varphi_{x_2}-\varphi_{x_1}) - \cos(\theta_2)\cos(\varphi_{y_1})\sin(\varphi_{x_2}-\varphi_{x_1})$$
$$+\sin(\theta_2)\sin(\varphi_{y_1})\cos(\varphi_{y_2})]z_1x_2 + [-\cos(\theta_2)\cos(\varphi_{y_1})\sin(\varphi_{y_2})\cos(\varphi_{x_2}-\varphi_{x_1})$$
$$+\sin(\theta_2)\cos(\varphi_{y_1})\sin(\varphi_{x_2}-\varphi_{x_1}) + \cos(\theta_2)\sin(\varphi_{y_1})\cos(\varphi_{y_2})]z_1y_2\Big) \qquad \text{(A23)}$$

In the case of a spring constraining body 1 to a body stationary in the inertial frame, the expression of the potential energy reduces to

$$\mathcal{U} = \tfrac{1}{2}k(X_1^2 + Y_1^2 + Z_1^2 + x_1^2 + y_1^2 + z_1^2 + x_0^2 + y_0^2 + z_0^2 + 2X_1[\cos(\theta_1)\cos(\varphi_{y_1})x_1$$
$$-\sin(\theta_1)\cos(\varphi_{y_1})y_1 + \sin(\varphi_{y_1})z_1 - x_0] + 2Y_1[\cos(\theta_1)\sin(\varphi_{y_1})\sin(\varphi_{x_1})x_1$$
$$+\sin(\theta_1)\cos(\varphi_{x_1})x_1 - \sin(\theta_1)\sin(\varphi_{y_1})\sin(\varphi_{x_1})y_1 + \cos(\theta_1)\cos(\varphi_{x_1})y_1$$
$$-\cos(\varphi_{y_1})\sin(\varphi_{x_1})z_1 - y_0] + 2Z_1[-\cos(\theta_1)\sin(\varphi_{y_1})\cos(\varphi_{x_1})x_1$$
$$+\sin(\theta_1)\sin(\varphi_{x_1})x_1 + \sin(\theta_1)\sin(\varphi_{y_1})\cos(\varphi_{x_1})y_1$$
$$+\cos(\theta_1)\sin(\varphi_{x_1})y_1 + \cos(\varphi_{y_1})\cos(\varphi_{x_1})z_1 - z_0] - 2\cos(\theta_1)\cos(\varphi_{y_1})x_1x_0$$
$$+2[-\cos(\theta_1)\sin(\varphi_{y_1})\sin(\varphi_{x_1}) - \sin(\theta_1)\cos(\varphi_{x_1})]x_1y_0$$
$$+2[\cos(\theta_1)\sin(\varphi_{y_1})\cos(\varphi_{x_1}) - \sin(\theta_1)\sin(\varphi_{x_1})]x_1z_0$$
$$+2\sin(\theta_1)\cos(\varphi_{y_1})y_1x_0 + 2[\sin(\theta_1)\sin(\varphi_{y_1})\sin(\varphi_{x_1}) - \cos(\theta_1)\cos(\varphi_{x_1})]y_1y_0$$
$$-2[\sin(\theta_1)\sin(\varphi_{y_1})\cos(\varphi_{x_1}) + \cos(\theta_1)\sin(\varphi_{x_1})]y_1z_0$$
$$-2\sin(\varphi_{y_1})z_1x_0 + 2\cos(\varphi_{y_1})\sin(\varphi_{x_1})z_1y_0 - 2\cos(\varphi_{y_1})\cos(\varphi_{x_1})z_1z_0) \qquad \text{(A24)}$$

The generalized forces are then

$$Q_{X_1} = -\frac{\partial \mathcal{U}}{\partial X_1} = -k[X_1 + \cos(\theta_1)\cos(\varphi_{y_1})x_1 - \sin(\theta_1)\cos(\varphi_{y_1})y_1$$
$$+\sin(\varphi_{y_1})z_1 - x_0], \qquad \text{(A25)}$$

$$Q_{Y_1} = -\frac{\partial \mathcal{U}}{\partial Y_1} = -k[Y_1 + \cos(\theta_1)\sin(\varphi_{y_1})\sin(\varphi_{x_1})x_1 + \sin(\theta_1)\cos(\varphi_{x_1})x_1$$
$$-\sin(\theta_1)\sin(\varphi_{y_1})\sin(\varphi_{x_1})y_1 + \cos(\theta_1)\cos(\varphi_{x_1})y_1$$
$$-\cos(\varphi_{y_1})\sin(\varphi_{x_1})z_1 - y_0], \qquad \text{(A26)}$$

$$Q_{Z_1} = -\frac{\partial \mathscr{U}}{\partial Z_1} = -k[Z_1 - \cos(\theta_1)\sin(\varphi_{y_1})\cos(\varphi_{x_1})x_1 + \sin(\theta_1)\sin(\varphi_{x_1})x_1$$
$$+ \sin(\theta_1)\sin(\varphi_{y_1})\cos(\varphi_{x_1})y_1 + \cos(\theta_1)\sin(\varphi_{x_1})y_1 +$$
$$\cos(\varphi_{y_1})\cos(\varphi_{x_1})z_1 - z_0] \tag{A27}$$

$$Q_{\varphi_{x_1}} = -\frac{\partial \mathscr{U}}{\partial \phi_{X_1}} = -k\{Y_1[\cos(\theta_1)\sin(\varphi_{y_1})\cos(\varphi_{x_1})x_1$$
$$- \sin(\theta_1)\sin(\varphi_{x_1})x_1 - \sin(\theta_1)\sin(\varphi_{y_1})\cos(\varphi_{x_1})y_1 - \cos(\theta_1)\sin(\varphi_{x_1})y_1$$
$$- \cos(\varphi_{y_1})\cos(\varphi_{x_1})z_1] + Z_1[\cos(\theta_1)\sin(\varphi_{y_1})\sin(\varphi_{x_1})x_1 + \sin(\theta_1)\cos(\varphi_{x_1})x_1$$
$$- \sin(\theta_1)\sin(\varphi_{y_1})\sin(\varphi_{x_1})y_1 + \cos(\theta_1)\cos(\varphi_{x_1})y_1 - \cos(\varphi_{y_1})\sin(\varphi_{x_1})z_1]$$
$$+ [-\cos(\theta_1)\sin(\varphi_{y_1})\cos(\varphi_{x_1}) + \sin(\theta_1)\sin(\varphi_{x_1})]x_1y_0$$
$$- [\cos(\theta_1)\sin(\varphi_{y_1})\sin(\varphi_{x_1}) + \sin(\theta_1)\cos(\varphi_{x_1})]x_1z_0$$
$$+ [\sin(\theta_1)\sin(\varphi_{y_1})\cos(\varphi_{x_1}) + \cos(\theta_1)\sin(\varphi_{x_1})]y_1y_0$$
$$+ [\sin(\theta_1)\sin(\varphi_{y_1})\sin(\varphi_{x_1}) - \cos(\theta_1)\cos(\varphi_{x_1})]y_1z_0$$
$$+ \cos(\varphi_{y_1})\cos(\varphi_{x_1})z_1y_0 + \cos(\varphi_{y_1})\sin(\varphi_{x_1})z_1z_0\} \tag{A28}$$

$$Q_{\varphi_{y_1}} = -\frac{\partial \mathscr{U}}{\partial \phi_{y_1}} = -k\{X_1[-\cos(\theta_1)\sin(\varphi_{y_1})x_1 + \sin(\theta_1)\sin(\varphi_{y_1})y_1$$
$$+ \cos(\varphi_{y_1})z_1] + Y_1[\cos(\theta_1)\cos(\varphi_{y_1})\sin(\varphi_{x_1})x_1 - \sin(\theta_1)\cos(\varphi_{y_1})\sin(\varphi_{x_1})y_1$$
$$+ \sin(\varphi_{y_1})\sin(\varphi_{x_1})z_1] + Z_1[-\cos(\theta_1)\cos(\varphi_{y_1})\cos(\varphi_{x_1})x_1$$
$$+ \sin(\theta_1)\cos(\varphi_{y_1})\cos(\varphi_{x_1})y_1 - \sin(\varphi_{y_1})\cos(\varphi_{x_1})z_1] + \cos(\theta_1)\sin(\varphi_{y_1})x_1x_0$$
$$- \cos(\theta_1)\cos(\varphi_{y_1})\sin(\varphi_{x_1})x_1y_0 + \cos(\theta_1)\cos(\varphi_{y_1})\cos(\varphi_{x_1})x_1z_0$$
$$- \sin(\theta_1)\sin(\varphi_{y_1})y_1x_0 + \sin(\theta_1)\cos(\varphi_{y_1})\sin(\varphi_{x_1})y_1y_0$$
$$- \sin(\theta_1)\cos(\varphi_{y_1})\cos(\varphi_{x_1})y_1z_0$$
$$- \cos(\varphi_{y_1})z_1x_0 - \sin(\varphi_{y_1})\sin(\varphi_{x_1})z_1y_0 + \sin(\varphi_{y_1})\cos(\varphi_{x_1})z_1z_0\}, \tag{A29}$$

$$Q_{\theta_1} = -\frac{\partial \mathscr{U}}{\partial \theta_1} = -k\{X_1[-\sin(\theta_1)\cos(\varphi_{y_1})x_1 - \cos(\theta_1)\cos(\varphi_{y_1})y_1]$$
$$+ Y_1[-\sin(\theta_1)\sin(\varphi_{y_1})\sin(\varphi_{x_1})x_1 + \cos(\theta_1)\cos(\varphi_{x_1})x_1$$
$$- \cos(\theta_1)\sin(\varphi_{y_1})\sin(\varphi_{x_1})y_1 - \sin(\theta_1)\cos(\varphi_{x_1})y_1]$$
$$+ Z_1[\sin(\theta_1)\sin(\varphi_{y_1})\cos(\varphi_{x_1})x_1 + \cos(\theta_1)\sin(\varphi_{x_1})x_1$$
$$+ \cos(\theta_1)\sin(\varphi_{y_1})\cos(\varphi_{x_1})y_1 - \sin(\theta_1)\sin(\varphi_{x_1})y_1] + \sin(\theta_1)\cos(\varphi_{y_1})x_1x_0$$
$$+ [\sin(\theta_1)\sin(\varphi_{y_1})\sin(\varphi_{x_1}) - \cos(\theta_1)\cos(\varphi_{x_1})]x_1y_0$$
$$- [\sin(\theta_1)\sin(\varphi_{y_1})\cos(\varphi_{x_1}) + \cos(\theta_1)\sin(\varphi_{x_1})]x_1z_0$$

$$+\cos(\theta_1)\cos(\varphi_{y_1})y_1x_0+[\cos(\theta_1)\sin(\varphi_{y_1})\sin(\varphi_{x_1})+\sin(\theta_1)\cos(\varphi_{x_1})]y_1y_0$$

$$+[-\cos(\theta_1)\sin(\varphi_{y_1})\cos(\varphi_{x_1})+\sin(\theta_1)\sin(\varphi_{x_1})]y_1z_0\}. \tag{A30}$$

A.3. RAYLEIGH DISSIPATION FUNCTION

Consider a linear viscous damper located between the two rigid bodies, with end points in point P_1 (located on body 1) and P_2 (on body 2). Assuming that the element in which the energy dissipation occurs moves together with body 1, the generalized damping forces can be computed from the Rayleigh dissipation function

$$\mathscr{F}=\tfrac{1}{2}\,c\overline{(\dot{P_2-P_1})}^{\mathrm{T}}\overline{(\dot{P_2-P_1})}, \tag{A31}$$

where $\overline{(\dot{P_2-P_1})}$ is the relative velocity of points P_1 and P_2 in the reference frame fixed to body 1.

Recalling equation (A11), the distance $\overline{(P_2-P_1)}$ can be expressed as

$$\overline{(P_2-P_1)}=\mathbf{R}_{3_1}\mathbf{R}_{2_1}\mathbf{R}_{1_1}\left[\mathbf{R}_{1_2}^{\mathrm{T}}\mathbf{R}_{2_2}^{\mathrm{T}}\mathbf{R}_{3_2}^{\mathrm{T}}\begin{Bmatrix}x_2\\y_2\\z_2\end{Bmatrix}+\begin{Bmatrix}X_2-X_1\\Y_2-Y_1\\Z_2-Z_1\end{Bmatrix}\right]-\begin{Bmatrix}x_1\\y_1\\z_1\end{Bmatrix}. \tag{A32}$$

By differentiating equation (A11) with respect to time and introducing it into equation (A31), the following expression of the Rayleigh dissipation function is readily obtained:

$$\mathscr{F}=\tfrac{1}{2}\,\dot{\mathbf{q}}^{\mathrm{T}}\mathbf{C}\dot{\mathbf{q}}, \tag{A33}$$

where

$$\mathbf{q}=[X_1\ \ Y_1\ \ Z_1\ \ \varphi_{x_1}\ \ \varphi_{y_1}\ \ \theta_1\ \ X_2\ \ Y_2\ \ Z_2\ \ \varphi_{x_2}\ \ \varphi_{y_2}\ \ \theta_2]^{\mathrm{T}},$$

$$\mathbf{C}=c\begin{bmatrix}
1 & 0 & 0 & -\mathbf{S}^{\mathrm{T}}\mathbf{O}_1 & -\mathbf{T}^{\mathrm{T}}\mathbf{O}_1 & -\mathbf{U}^{\mathrm{T}}\mathbf{O}_1 & -1 & 0 & 0 & -\mathbf{V}^{\mathrm{T}}\mathbf{O}_1 & -\mathbf{W}^{\mathrm{T}}\mathbf{O}_1 & -\mathbf{P}^{\mathrm{T}}\mathbf{O}_1\\
 & 1 & 0 & -\mathbf{S}^{\mathrm{T}}\mathbf{O}_2 & -\mathbf{T}^{\mathrm{T}}\mathbf{O}_2 & -\mathbf{U}^{\mathrm{T}}\mathbf{O}_2 & 0 & -1 & 0 & -\mathbf{V}^{\mathrm{T}}\mathbf{O}_2 & -\mathbf{W}^{\mathrm{T}}\mathbf{O}_2 & -\mathbf{P}^{\mathrm{T}}\mathbf{O}_2\\
 & & 1 & -\mathbf{S}^{\mathrm{T}}\mathbf{O}_3 & -\mathbf{T}^{\mathrm{T}}\mathbf{O}_3 & -\mathbf{U}^{\mathrm{T}}\mathbf{O}_3 & 0 & 0 & -1 & -\mathbf{V}^{\mathrm{T}}\mathbf{O}_3 & -\mathbf{W}^{\mathrm{T}}\mathbf{O}_3 & -\mathbf{P}^{\mathrm{T}}\mathbf{O}_3\\
 & & & \mathbf{S}^{\mathrm{T}}\mathbf{S} & \mathbf{T}^{\mathrm{T}}\mathbf{S} & \mathbf{U}^{\mathrm{T}}\mathbf{S} & \mathbf{O}_1^{\mathrm{T}}\mathbf{S} & \mathbf{O}_2^{\mathrm{T}}\mathbf{S} & \mathbf{O}_3^{\mathrm{T}}\mathbf{S} & \mathbf{V}^{\mathrm{T}}\mathbf{S} & \mathbf{W}^{\mathrm{T}}\mathbf{S} & \mathbf{P}^{\mathrm{T}}\mathbf{S}\\
 & & & & \mathbf{T}^{\mathrm{T}}\mathbf{T} & \mathbf{U}^{\mathrm{T}}\mathbf{T} & \mathbf{O}_1^{\mathrm{T}}\mathbf{T} & \mathbf{O}_2^{\mathrm{T}}\mathbf{T} & \mathbf{O}_3^{\mathrm{T}}\mathbf{T} & \mathbf{V}^{\mathrm{T}}\mathbf{T} & \mathbf{W}^{\mathrm{T}}\mathbf{T} & \mathbf{P}^{\mathrm{T}}\mathbf{T}\\
 & & & & & \mathbf{U}^{\mathrm{T}}\mathbf{U} & \mathbf{O}_1^{\mathrm{T}}\mathbf{U} & \mathbf{O}_2^{\mathrm{T}}\mathbf{U} & \mathbf{O}_3^{\mathrm{T}}\mathbf{U} & \mathbf{V}^{\mathrm{T}}\mathbf{U} & \mathbf{W}^{\mathrm{T}}\mathbf{U} & \mathbf{P}^{\mathrm{T}}\mathbf{U}\\
 & & & & & & 1 & 0 & 0 & \mathbf{V}^{\mathrm{T}}\mathbf{O}_1 & \mathbf{W}^{\mathrm{T}}\mathbf{O}_1 & \mathbf{P}^{\mathrm{T}}\mathbf{O}_1\\
 & & & & & & & 1 & 0 & \mathbf{V}^{\mathrm{T}}\mathbf{O}_2 & \mathbf{W}^{\mathrm{T}}\mathbf{O}_2 & \mathbf{P}^{\mathrm{T}}\mathbf{O}_2\\
 & & & & & & & & 1 & \mathbf{V}^{\mathrm{T}}\mathbf{O}_3 & \mathbf{W}^{\mathrm{T}}\mathbf{O}_3 & \mathbf{P}^{\mathrm{T}}\mathbf{O}_3\\
 & & & \textit{Symm.} & & & & & & \mathbf{V}^{\mathrm{T}}\mathbf{V} & \mathbf{W}^{\mathrm{T}}\mathbf{V} & \mathbf{P}^{\mathrm{T}}\mathbf{V}\\
 & & & & & & & & & & \mathbf{W}^{\mathrm{T}}\mathbf{W} & \mathbf{P}^{\mathrm{T}}\mathbf{W}\\
 & & & & & & & & & & & \mathbf{P}^{\mathrm{T}}\mathbf{P}
\end{bmatrix}$$

$$\mathbf{S} = \mathbf{R}_{3_1}\mathbf{R}_{2_1}\boldsymbol{\gamma}_1\left[\mathbf{R}_{1_2}^{\mathrm{T}}\mathbf{R}_{2_2}^{\mathrm{T}}\mathbf{R}_{3_2}^{\mathrm{T}}\begin{Bmatrix}x_2\\y_2\\z_2\end{Bmatrix} + \begin{Bmatrix}X_2 - X_1\\Y_2 - Y_1\\Z_2 - Z_1\end{Bmatrix}\right],$$

$$\mathbf{T} = \mathbf{R}_{3_1}\boldsymbol{\beta}_1\mathbf{R}_{1_1}\left[\mathbf{R}_{1_2}^{\mathrm{T}}\mathbf{R}_{2_2}^{\mathrm{T}}\mathbf{R}_{3_2}^{\mathrm{T}}\begin{Bmatrix}x_2\\y_2\\z_2\end{Bmatrix} + \begin{Bmatrix}X_2 - X_1\\Y_2 - Y_1\\Z_2 - Z_1\end{Bmatrix}\right],$$

$$\mathbf{U} = \boldsymbol{\alpha}_1\mathbf{R}_{2_1}\mathbf{R}_{1_1}\left[\mathbf{R}_{1_2}^{\mathrm{T}}\mathbf{R}_{2_2}^{\mathrm{T}}\mathbf{R}_{3_2}^{\mathrm{T}}\begin{Bmatrix}x_2\\y_2\\z_2\end{Bmatrix} + \begin{Bmatrix}X_2 - X_1\\Y_2 - Y_1\\Z_2 - Z_1\end{Bmatrix}\right],$$

$$\mathbf{V} = \mathbf{R}_{3_1}\mathbf{R}_{2_1}\mathbf{R}_{1_1}\boldsymbol{\gamma}_2^{\mathrm{T}}\mathbf{R}_{2_2}^{\mathrm{T}}\mathbf{R}_{3_2}^{\mathrm{T}}\begin{Bmatrix}x_2\\y_2\\z_2\end{Bmatrix},$$

$$\mathbf{W} = \mathbf{R}_{3_1}\mathbf{R}_{2_1}\mathbf{R}_{1_1}\mathbf{R}_{1_2}^{\mathrm{T}}\boldsymbol{\beta}_2{}^{\mathrm{T}}\mathbf{R}_{3_2}^{\mathrm{T}}\begin{Bmatrix}x_2\\y_2\\z_2\end{Bmatrix},$$

$$\mathbf{P} = \mathbf{R}_{3_1}\mathbf{R}_{2_1}\mathbf{R}_{1_1}\mathbf{R}_{1_2}^{\mathrm{T}}\mathbf{R}_{2_2}^{\mathrm{T}}\boldsymbol{\alpha}_2{}^{\mathrm{T}}\begin{Bmatrix}x_2\\y_2\\z_2\end{Bmatrix},$$

$$\boldsymbol{\alpha}_i = \begin{bmatrix} -\sin(\theta_i) & \cos(\theta_i) & 0\\ -\cos(\theta_i) & -\sin(\theta_i) & 0\\ 0 & 0 & 0\end{bmatrix},$$

$$\boldsymbol{\beta}_i = \begin{bmatrix} -\sin(\varphi_{y_i}) & 0 & -\cos(\varphi_{y_i})\\ 0 & 0 & 0\\ \cos(\varphi_{y_i}) & 0 & -\sin(\varphi_{y_i})\end{bmatrix},$$

$$\boldsymbol{\gamma}_i = \begin{bmatrix}0 & 0 & 0\\ 0 & -\sin(\varphi_{x_i}) & \cos(\varphi_{x_i})\\ 0 & -\cos(\varphi_{x_i}) & -\sin(\varphi_{x_i})\end{bmatrix},$$

$$\mathbf{O} = \mathbf{R}_{3_1}\mathbf{R}_{2_1}\mathbf{R}_{1_1}$$

and $\mathbf{O}_1$, $\mathbf{O}_2$, and $\mathbf{O}_3$ are the first, second and third columns of matrix $\mathbf{O}$ respectively.

In the case of a damper located between point P_1 (located on body 1) and point P_0 fixed to the inertial frame, assuming that the element in which the energy dissipation occurs is stationary in the latter, the Rayleigh dissipation function is

$$\mathscr{F} = \tfrac{1}{2}c\,\overline{(\mathrm{P}_1 - \mathrm{P}_0)}^{\mathrm{T}}\,\overline{(\mathrm{P}_1 - \mathrm{P}_0)} \tag{A34}$$

where the relative velocity of points P_1 and P_0 is referred to the inertial frame.

Remembering equation (A11), the distance $(\overline{P_1 - P_0})$ can be expressed as

$$(\overline{P_1 - P_0}) = \mathbf{R}_{1_1}^{T}\mathbf{R}_{2_1}^{T}\mathbf{R}_{3_1}^{T}\begin{Bmatrix} x_1 \\ y_1 \\ z_1 \end{Bmatrix} + \begin{Bmatrix} X_1 \\ Y_1 \\ Z_1 \end{Bmatrix} - \begin{Bmatrix} x_0 \\ y_0 \\ z_0 \end{Bmatrix}. \tag{A35}$$

Operating as above, the vector of the generalized coordinates is

$$\mathbf{q} = [X_1 \quad Y_1 \quad Z_1 \quad \varphi_{x_1} \quad \varphi_{x_1} \quad \theta_1]^{T},$$

and matrix $\mathbf{C}$ is easily computed

$$\mathbf{C} = c\begin{bmatrix} 1 & 0 & 0 & \mathbf{V}^{T}\mathbf{I}_1 & \mathbf{W}^{T}\mathbf{I}_1 & \mathbf{P}^{T}\mathbf{I}_1 \\ & 1 & 0 & \mathbf{V}^{T}\mathbf{I}_2 & \mathbf{W}^{T}\mathbf{I}_2 & \mathbf{P}^{T}\mathbf{I}_2 \\ & & 1 & \mathbf{V}^{T}\mathbf{I}_3 & \mathbf{W}^{T}\mathbf{I}_3 & \mathbf{P}^{T}\mathbf{I}_3 \\ & & & \mathbf{V}^{T}\mathbf{V} & \mathbf{W}^{T}\mathbf{V} & \mathbf{P}^{T}\mathbf{V} \\ & \text{Symm.} & & & \mathbf{W}^{T}\mathbf{W} & \mathbf{P}^{T}\mathbf{W} \\ & & & & & \mathbf{P}^{T}\mathbf{P} \end{bmatrix},$$

where

$$\mathbf{V} = \boldsymbol{\gamma}_1^{T}\mathbf{R}_{2_1}^{T}\mathbf{R}_{3_1}^{T}\begin{Bmatrix} x_1 \\ y_1 \\ z_1 \end{Bmatrix}, \qquad \mathbf{W} = \mathbf{R}_{1_1}^{T}\boldsymbol{\beta}_1^{T}\mathbf{R}_{3_1}^{T}\begin{Bmatrix} x_1 \\ y_1 \\ z_1 \end{Bmatrix}, \qquad \mathbf{P} = \mathbf{R}_{1_1}^{T}\mathbf{R}_{2_1}^{T}\boldsymbol{\alpha}_1^{T}\begin{Bmatrix} x_1 \\ y_1 \\ z_1 \end{Bmatrix}$$

and $\mathbf{I}_1$, $\mathbf{I}_2$, and $\mathbf{I}_3$ are the first, second and third columns of the identity matrix, respectively.

In both cases, the generalized forces due to damping to be inserted in the equations of motion are

$$\mathbf{Q} = -\mathbf{C}\dot{\mathbf{q}}. \tag{A36}$$

APPENDIX B: NOMENCLATURE

c	damping coefficient
k	stiffness
i	imaginary unit ($i = \sqrt{-1}$)
m	mass
$\mathbf{q}$	coordinate vector
t	time
$\mathbf{C}$	damping matrix
$\mathbf{F}$	unbalance force vector
$\mathscr{F}$	Rayleigh dissipation function
$\mathbf{G}$	gyroscopic matrix
$\mathbf{K}$	stiffness matrix
J	moment of inertia
$\mathbf{M}$	mass matrix
$\mathbf{R}$	rotation matrix
$\mathscr{T}$	kinetic energy

Q	generalized force
$\mathcal{U}$	potential energy
ε	eccentricity
ζ	damping ratio
λ	whirl speed
ω	spin speed
Ω	angular velocity